Institute of Polar Studies

Report No. 66

Meltwater Storage in a Temperate Glacier Burroughs Glacier, Southeast Alaska

by

Grahame J. Larson

Institute of Polar Studies
and
Department of Geology and Mineralogy

1978

The Ohio State University
Institute of Polar Studies
Columbus, Ohio 43210

INSTITUTE OF POLAR STUDIES

Report No. 66

MELTWATER STORAGE IN A TEMPERATE GLACIER

BURROUGHS GLACIER, SOUTHEAST ALASKA

by

Grahame J. Larson

Institute of Polar Studies

and

Department of Geology and Mineralogy
The Ohio State University

1978

Institute of Polar Studies
The Ohio State University
Columbus, Ohio 43210

Dr. Grahame J. Larson is now at:

Department of Geology
Michigan State University
East Lansing, Michigan 48824

Copies of this and other reports of the
Institute of Polar Studies are available from:

Institute of Polar Studies
The Ohio State University
125 South Oval Mall
Columbus, Ohio 43210
614-422-6531

ABSTRACT

Burroughs Glacier is a wasting mass of neoglacial ice in the northeastern part of the Glacier Bay National Monument, Alaska. The entire glacier covers approximately 26 km^2 and consists of two tongues both of which flow from a central ice divide. The highest point on the glacier (475 m) lies on the divide and is well below the equilibrium line. The average annual rate of downwastage of the ice surface is approximately 3.7 m.

During the summer of 1973, a hydrologic study was made of the eastern tongue of the glacier (13.9 km^2). The study involved calculating the inflow and outflow of meltwater in the tongue for the purpose of analyzing the storage characteristics of glacier ice. The results of the investigation show that during a four-day period of generally clear skies and mild temperatures, approximately 17.8 cm of water was produced on the glacier surface by melting. The runoff recorded during this period, however, was only 14.2 cm which suggests that at least 3.6 cm of meltwater was retained within the glacier tongue. Most of this meltwater storage appears to occur within channels and open fractures in the ice itself.

Analysis of the relationship between the storage in the tongue sub-basins and the runoff in the streams draining the sub-basins indicates that the average basin lag from the glacier to the channel control is approximately three hours. There appears to be no observable relationship between the average basin lag and the area of the sub-basin being drained.

ACKNOWLEDGEMENT

Field work for this investigation was conducted during the summers of 1972 and 1973, and was made possible by two Penrose Bequest Research Grants (No. 1587-72 and 1726-73) from the Geological Society of America. Support was also given by The Ohio State University Department of Geology and Mineralogy, the Institute of Polar Studies, and the Society of Sigma Xi. Invaluable logistical support was provided by the National Park Service, Glacier Bay National Monument, Alaska.

My sincerest thanks are extended to Dr. Wayne A. Pettyjohn and Dr. Richard P. Goldthwait, professors of geology at The Ohio State University, for their guidance both in the field and during the analyses of the collected data. Special thanks are also due to Dr. Charles E. Corbató for his assistance in developing the computer programs necessary for this project, and to Peter J. Anderson, Assistant Director of the Institute of Polar Studies, who edited the manuscript. Ms. Loretta Knutson and Mrs. Jean Cothran typed the final manuscript.

Special thanks is given to Donna Larson. Her help and encouragement in the field were invaluable.

TABLE OF CONTENTS

ILLUSTRATIONS

ILLUSTRATIONS (Continued)

TABLES

INTRODUCTION

Within the past few decades, hydrologists and glaciologists have become increasingly aware of the importance of glaciers as potential water resources. This is particularly true in the mountainous and high latitude regions of the world where rapid industrial and agricultural developments are taking place. For example, both the Swiss and the French have already tunnelled under glaciers and successfully diverted subglacial streams for hydroelectric power generation (Cottier and others, 1957; Vivian, 1970). Power and water supply projects utilizing glacial runoff are presently also being considered by both the Norwegian Water Resources and Electricity Board (Østrem, 1971; 1974) and the Canadian Department of Energy, Mines, and Resources (Løken, 1970; Ommanny, 1970). In addition, several glaciers within the United States and the Soviet Union are being evaluated as potential water supplies (Meier, 1969; Meier and others, 1971; Tangborn, 1966; Tangborn and others, 1971; Post and others, 1971; Kotlyakov, 1973).

A thorough understanding of the occurrence, distribution, and behavior of liquid water in ice is undoubtedly necessary if glaciers are to be effectively developed as natural resources. Already, direct observations (Sharp, 1951; Colbeck, 1971) and tracer experiments (Stenborg, 1973; Krimmel and others, 1973) have provided much valuable insight into the drainage systems operating on or just beneath the glacier surface. As yet, however, little research has been directed towards understanding the storage characteristics of glacier ice. This is because it is almost impossible to study the inaccessible openings within the ice from the exterior of the glacier or by remote sensing from its surface.

During the summer of 1973, the water balance for part of Burroughs Glacier, in southeastern Alaska, was analyzed to determine indirectly some of the storage characteristics of glacier ice. The results of the investigation are presented in this report. In the chapter entitled "Inflow", the areal variability of melt due to global radiation alone is analyzed for the purpose of approximating the melt over the glacier surface during a nearly cloudless four-day period. In the chapter entitled "Outflow", the runoff of meltwater from the glacier is estimated for the same four-day period. Finally, in the chapter entitled "Meltwater Storage", the storage characteristics of the glacier are investigated by comparing the inflow and outflow records for the four days.

Burroughs Glacier is well suited for hydrologic study. It is confined on all sides by bedrock and is drained by only a few outlet streams. The surface of the glacier lies entirely below the equilibrium line and, by late summer, is at the pressure melting point throughout. In addition, a plethora of background data on the glacial history, geology, and glaciology of the glacier and surrounding area is also available from several investigations made over the past twenty years (Taylor, 1962; Goldthwait, 1966; Mickelson; 1971).

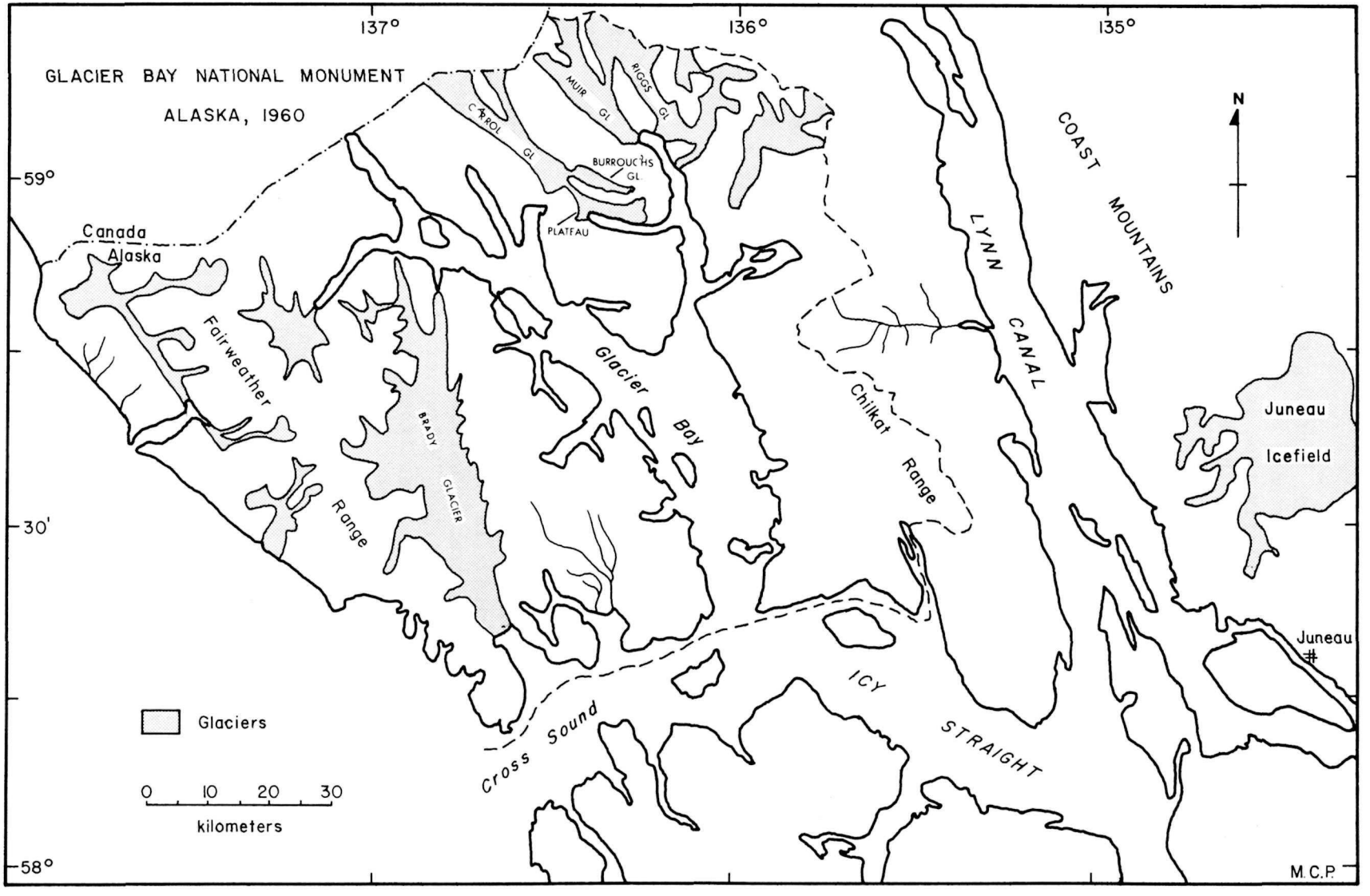

Figure 1. Location of Burroughs Glacier.

PHYSICAL SETTING OF BURROUGHS GLACIER

Burroughs Glacier (59' 00" N. Lat., 136' 20" Long.) is a wasting mass of neoglacial ice confined to a valley just north of Wachusett Inlet in the northeastern part of Glacier Bay National Monument, Alaska. The glacier is approximately 13 km.long and 1.2 to 3 km. wide, and covers 26 sq. km. An index map of the glacier and surrounding area is presented in Figure 1.

The highest point on the glacier surface (475 m) lies on an ice divide that separates the glacier into two distinct tongues. The eastern tongue (Fig. 2) is approximately 6.8 km. long and covers 13.9 sq. km. At the glacier divide, the tongue is about 2.2 km. wide, but down glacier it widens to about 3 km. The direction of ice flow in the tongue is easterly. The western tongue of the glacier flows in the opposite direction. It is approximately 6.2 km. long, covers 12.1 sq. km. and descends to an elevation of 150 m. Unlike the eastern tongue, it becomes narrower down glacier and is about 1.0 km. wide near its terminus.

General Characteristics of the Basin

In this investigation only the eastern tongue of Burroughs Glacier and its surrounding basin are considered. The basin (Fig. 2) is approximately 27.2 sq. km. and is bounded on the north by Minnesota Ridge, on the east by the Curtis Hills, and on the south by the Bruce Hills. The western boundary of the basin is defined by the ice divide separating Burroughs Glacier into two tongues.

Three streams within the basin (Burroughs River, Bob Creek, and Gull Creek) drain meltwater from the glacier. Prior to 1972, a fourth stream (John Creek), also drained meltwater, but is has since diverted under the ice and dried up.

Geology

The bedrock underlying the basin is predominantly a series of metamorphosed shales and limestones, intruded by diorite and granodiorite stocks (Mackevett and others, 1971). The metasediments are Paleozoic in age and underlie much of the eastern half of the basin. The western half is underlain primarily by stocks of Cretaceous age.

Surficial deposits mask much of the bedrock in the basin. These recent deposits, described and mapped by Mickelson (1971), consist largely of till, sand, and gravel. The till is generally sandy and ranges in thickness from a veneer of scattered boulders to more than 25 m. The sand and gravel deposits are mostly kame terraces or outwash of Hysithermal and Recent age. The gravel is generally medium to coarse, and, in some parts of the basin, may be tens of meters thick.

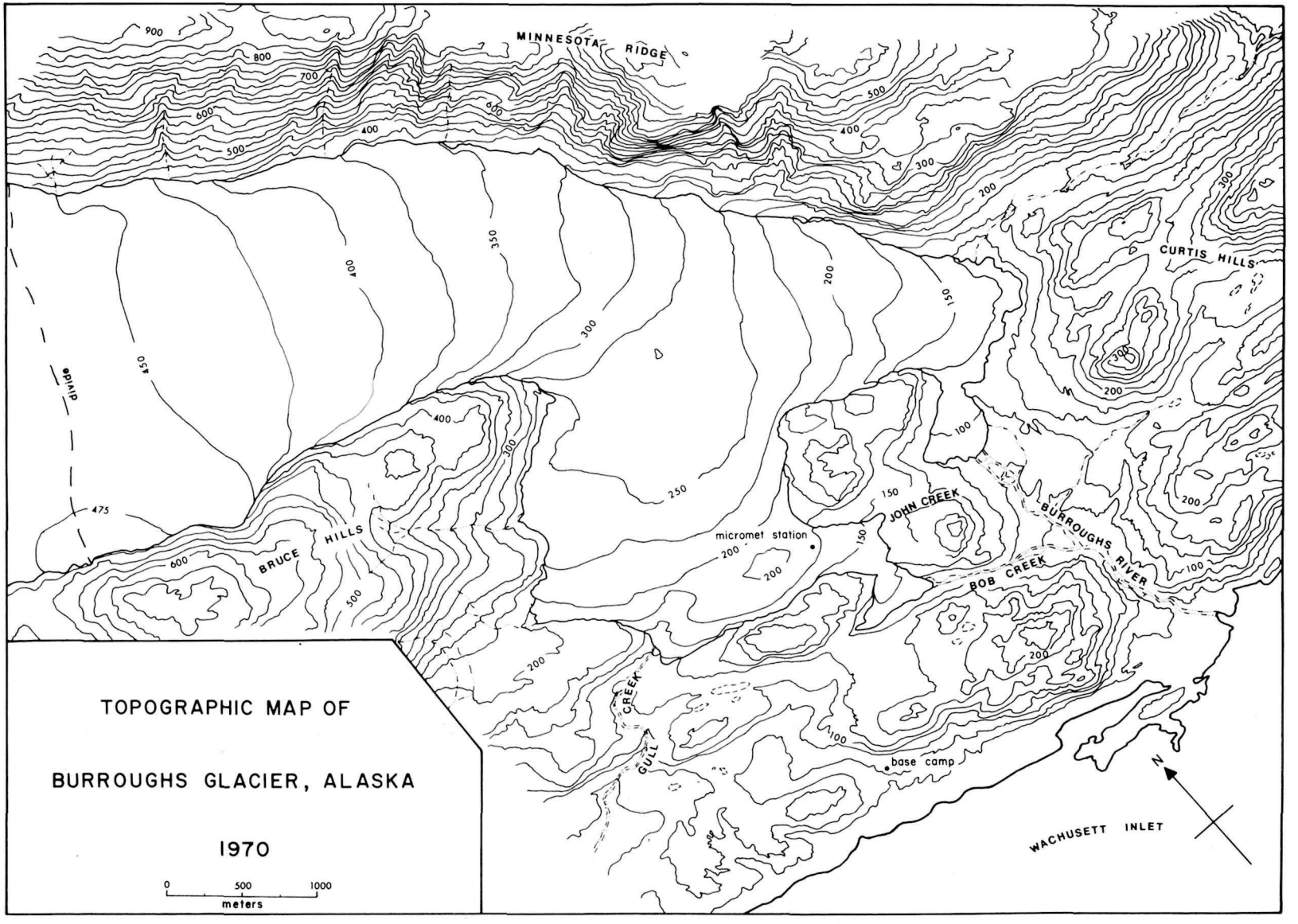
MINNESOTA RIDGE
CURTIS HILLS
BRUCE HILLS
DIVIDE
micromet station
JOHN CREEK
BURROUGHS RIVER
BOB CREEK
GULL CREEK
base camp
WACHUSETT INLET
N
TOPOGRAPHIC MAP OF
BURROUGHS GLACIER, ALASKA
1970
0 500 1000
meters

Fig. 2

Climate

The climate of Glacier Bay has been summarized by Loewe (1966) and McKenzie (1968, 1970). It is generally maritime and characterized by small daily and seasonal temperature ranges, many long periods of fog and cloudiness, high relative humidity, and abundant precipitation (200 to 400 cm). No permanent meteorological stations have ever been maintained at Burroughs Glacier, but records have been kept by field parties during the summers of 1960 (Taylor, 1962); of 1969 and 1970 (Michelson, 1971; Larson, 1977); and of 1972 and 1973 (this report). These records show that summers at Burroughs Glacier are generally typified by long periods of heavy overcast, abundant rainfall (200 mm month^{-1}), and temperatures around 10°C. $\pm$ 5°.

Glaciology

According to Ahlmann's (1948) dynamic classification scheme, Burroughs Glacier is a "dead glacier". It receives no supply of new ice each year, and any movement within the glacier is due mainly to the slope of the glacier surface.

Glacier flow. The magnitude and direction of ice flow in Burroughs Glacier from August 1972 to August 1973 is shown in Figure 3. During this period, ice flow ranged from just over 6 m yr^{-1} at the narrowest part of the glacier tongue to less than 0.2 m yr^{-1} near the glacier terminus. The direction of ice movement was not always parallel with the slope of the glacier surface, suggesting that flow is somewhat influenced by the subglacial topography.

Ice temperature. No measurements were made of the thermal regimen of the glacier, however, it is assumed to be temperate (Taylor, 1962; Mickelson, 1971). This assumption is supported by seismic "P" wave velocities measured in the ice during July and August of 1973. The velocities ranged from 3,580 to 3,660 m sec^{-1} which falls well within the range suggested by Robin (1958) for temperate glacier ice.

Ice structures. The surficial structural features of Burroughs Glacier have been studied and described by Taylor (1962) and include foliation, banding, fractures, and crevasses. The foliation on the surface is most pronounced on the higher part of the glacier. It consists of alternating layers of bubble-rich and bubble-free ice, and is generally parallel to Minnesota Ridge. The banding, on the other hand, is due to variations in the fine dirt content of the ice, and is most evident near the glacier terminus, where the bands form lobate patterns parallel to the glacier margin. The ice crystals on the glacier surface generally range from 0.1 to 5 cm in diameter.

A map of the crevasses on Burroughs Glacier is shown in Figure 4. It is apparent from the map that the crevasses occur in two principal patterns. On the higher part of the glacier they form a transverse pattern, but down glacier, the pattern is more longitudinal. Most of the crevasses are vertical and generally less than 30 cm in width and 10 m in depth. The fractures in the ice occur over most of the glacier surface and appear to be shear faults with little if any normal separation.

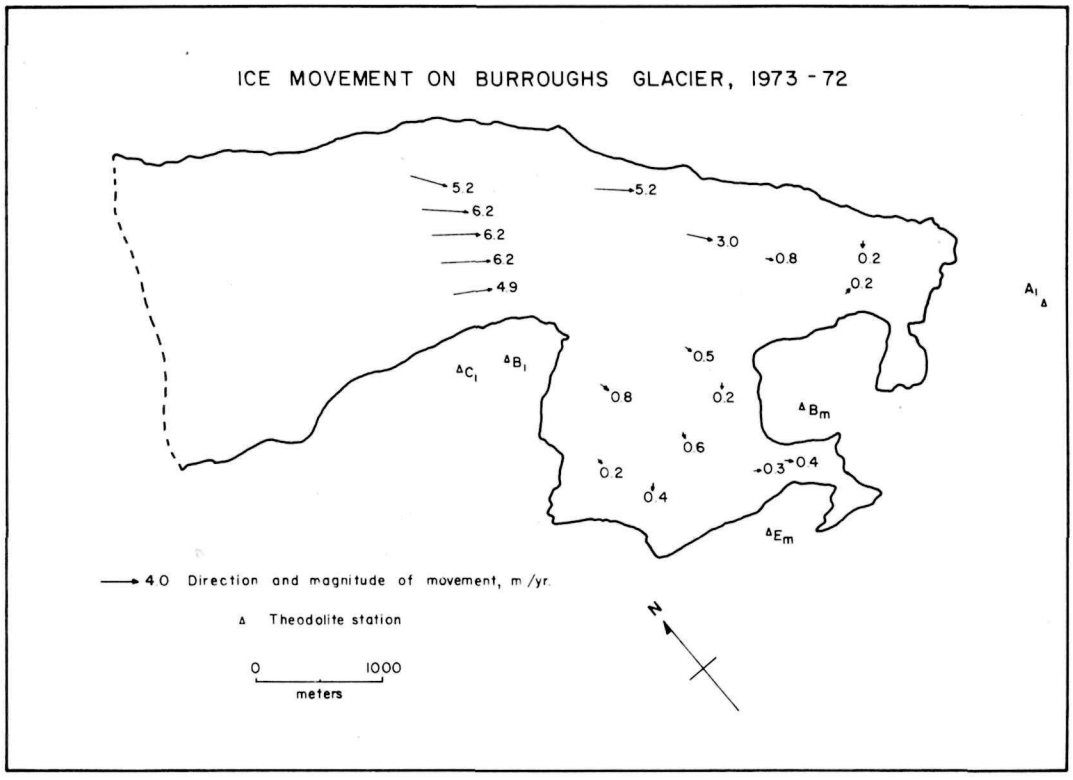
ICE MOVEMENT ON BURROUGHS GLACIER, 1973 - 72
5.2
5.2
6.2
6.2
6.2
4.9
3.0
0.8
0.2
0.2
0.5
0.8
0.2
0.6
0.2
0.4
0.3
0.4
A_1
B_1
C_1
B_m
E_m
4.0 Direction and magnitude of movement, m /yr.
Theodolite station
0
1000
meters
N

Fig. 3

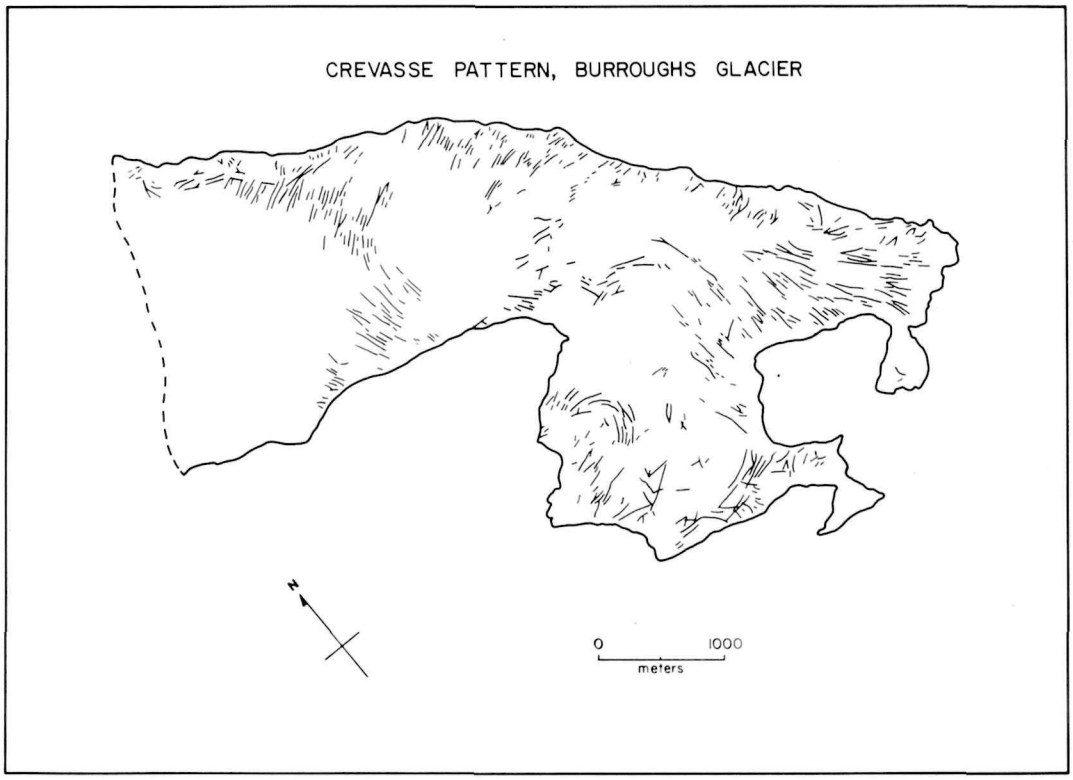
CREVASSE PATTERN, BURROUGHS GLACIER
N
0
1000
meters

Fig. 4

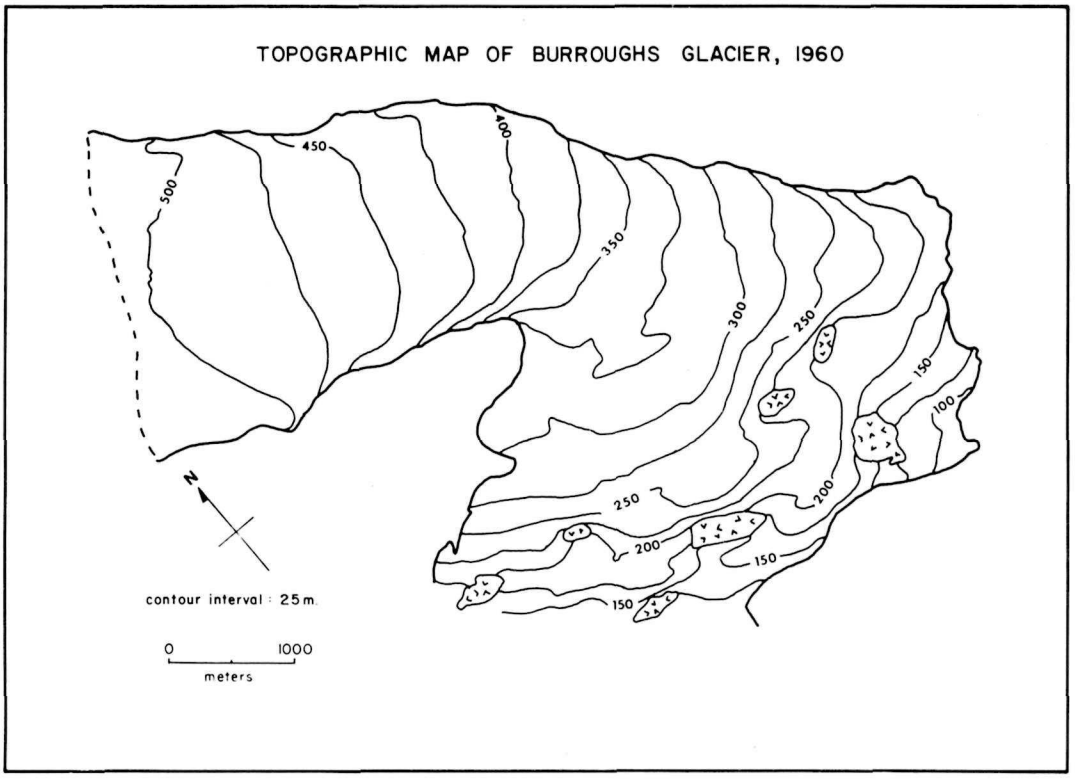
TOPOGRAPHIC MAP OF BURROUGHS GLACIER, 1960
500
450
400
350
300
250
150
100
250
200
200
150
150
N
contour interval : 25 m.
0
1000
meters

Fig. 5

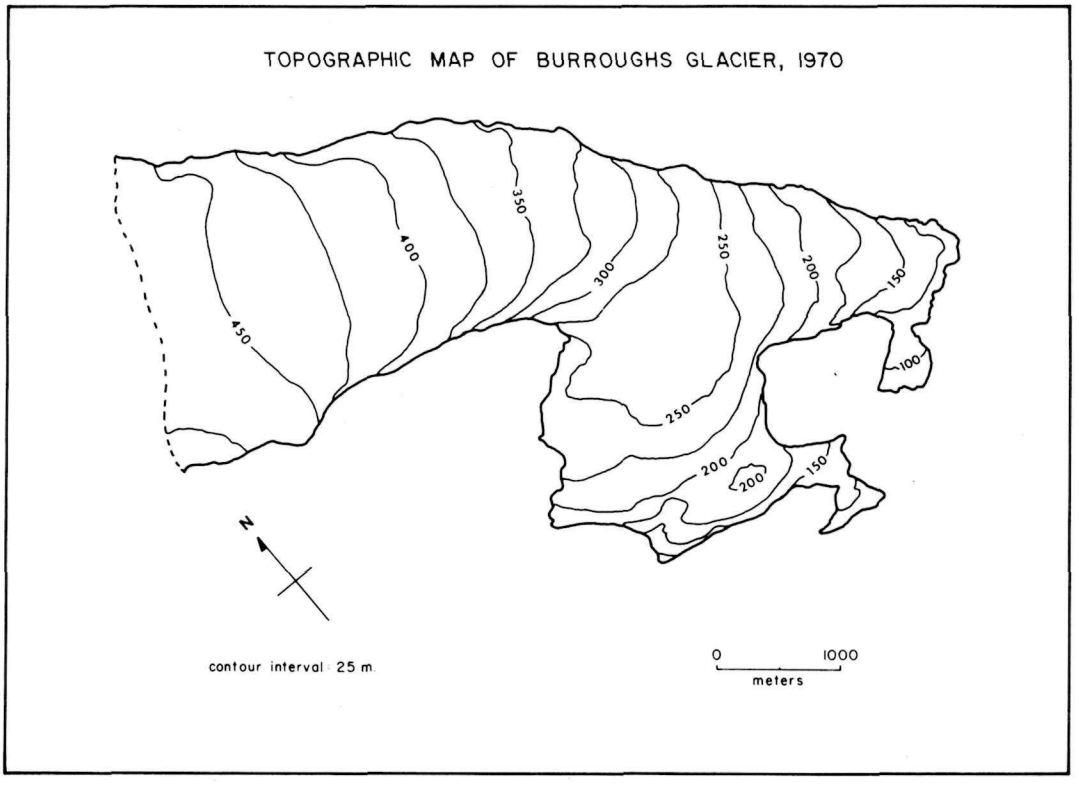
TOPOGRAPHIC MAP OF BURROUGHS GLACIER, 1970
450
400
350
300
250
200
150
100
250
200
200
150
N
contour interval : 25 m.
0
1000
meters

Fig. 6

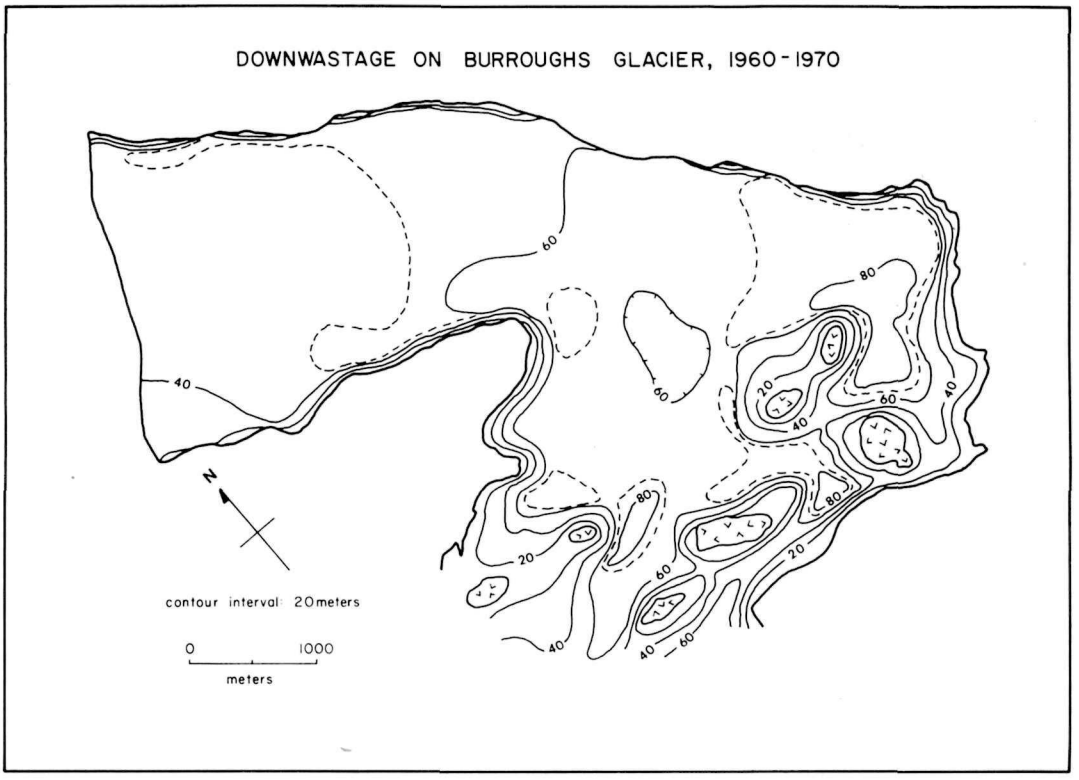
DOWNWASTAGE ON BURROUGHS GLACIER, 1960-1970
40
60
80
20
N
contour interval 20 meters
0
1000
meters

Fig. 7

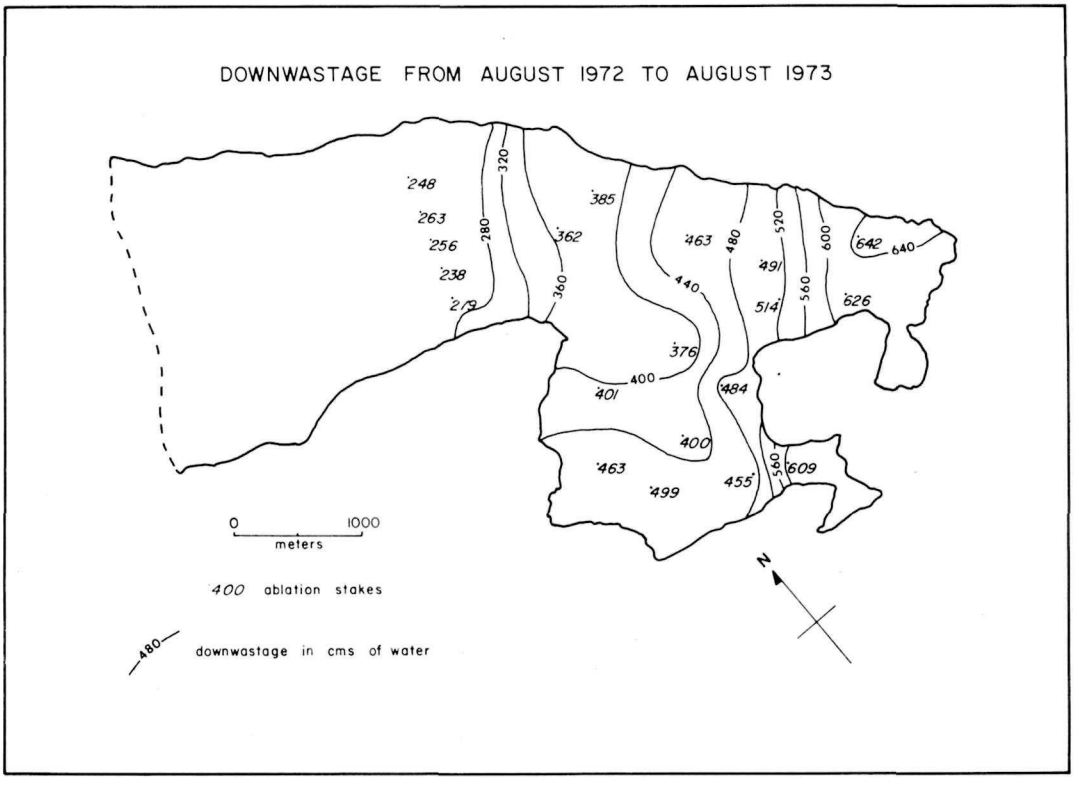
DOWNWASTAGE FROM AUGUST 1972 TO AUGUST 1973
248
263
256
238
320
280
360
385
362
463
480
520
600
642
640
491
440
514
560
626
376
400
401
484
400
463
499
455
560
609
0
1000
meters
400 ablation stakes
480
downwastage in cms of water
N

Fig. 8

Downwastage. Since 1891, numerous maps have been published of the Burroughs Glacier area. The earliest maps, prepared by Cushing (1891) and Reid (1892), do not show Burroughs Glacier as it appears today, but instead, reveal an ice plateau nearly 750 m thick which covers approximately 250 sq. km. (the Cushing Glacier). During the last 85 years, this plateau has downwasted as much as 8 m per year and has separated into a number of smaller glaciers (Burroughs Glacier, Plateau Glacier, Carrol Glacier). The history of this deglaciation has been described in detail by Field (1947), Taylor (1962), Goldthwait (1966), and Mickelson (1971).

A quick comparison of a 1960 and 1970 map of Burroughs Glacier (Figs. 5 and 6) confirms that deglaciation is still continuing. In ten years alone, the glacier surface has melted down as much as 9 m yr^{-1}, while the ice margin has retreated in some places as much as 0.2 km yr^{-1}.

Total downwastage from 1960 to 1970 is shown in Figure 7. The map was constructed by calculating the difference between the 1960 and 1970 glacier surface. It is evident from the map that downwastage is greatest near the glacier terminus (80 m), and least at the glacier divide (40 m). The total volume of ice lost during this period, determined by calculating areas within contours, was approximately $1.0 \times 10^9 m^3$. This is equivalent to an average annual lowering of 5.6 m.

For the period September 1972 to September 1973, ablation stakes were used to record downwastage of the glacier surface (Fig. 8). The measured rates of surface lowering ranged from 2.65 m yr^{-1} at the uppermost stake to 7.13 m yr^{-1} at the lowermost stake. The volume of ice lost during this period was approximately $5.1 \times 10^7 m^3$. The average rate of lowering was about 3.7 m yr^{-1}.

The relationship between the rate of downwastage and altitude at each stake is shown in Figure 9. The data clearly indicate that downwastage decreases slowly, but irregularly, with increasing altitude. A straight line fitted to the data points by least-squares regression suggests that downwastage decreases approximately 1.2 m for every 100 m increase in altitude. The equation of the line would also suggest that at an altitude of 617 m, downwastage would be zero. The noticeable scatter of points about the line is undoubtedly due to spacial variances in ice density, roughness, exposure and surface albedo.

Surface Albedo. When global radiation (I_g) falls on a surface, a certain amount is absorbed; the remainder (I_r) is reflected back into the atmosphere. The albedo (α) of the surface, generally expressed as a percent, is the ratio of the neglected radiation to global radiation, i.e.

$$\alpha = {}^{I}r/I_g \times 100 .$$

Figure 10 shows the surface albedo of Burroughs Glacier recorded at 17 stations during the early afternoon of August 15, 1973. At each station the incoming global radiation was measured with an Epply pyronometer placed in a level position on the glacier surface. The reflected radiation was

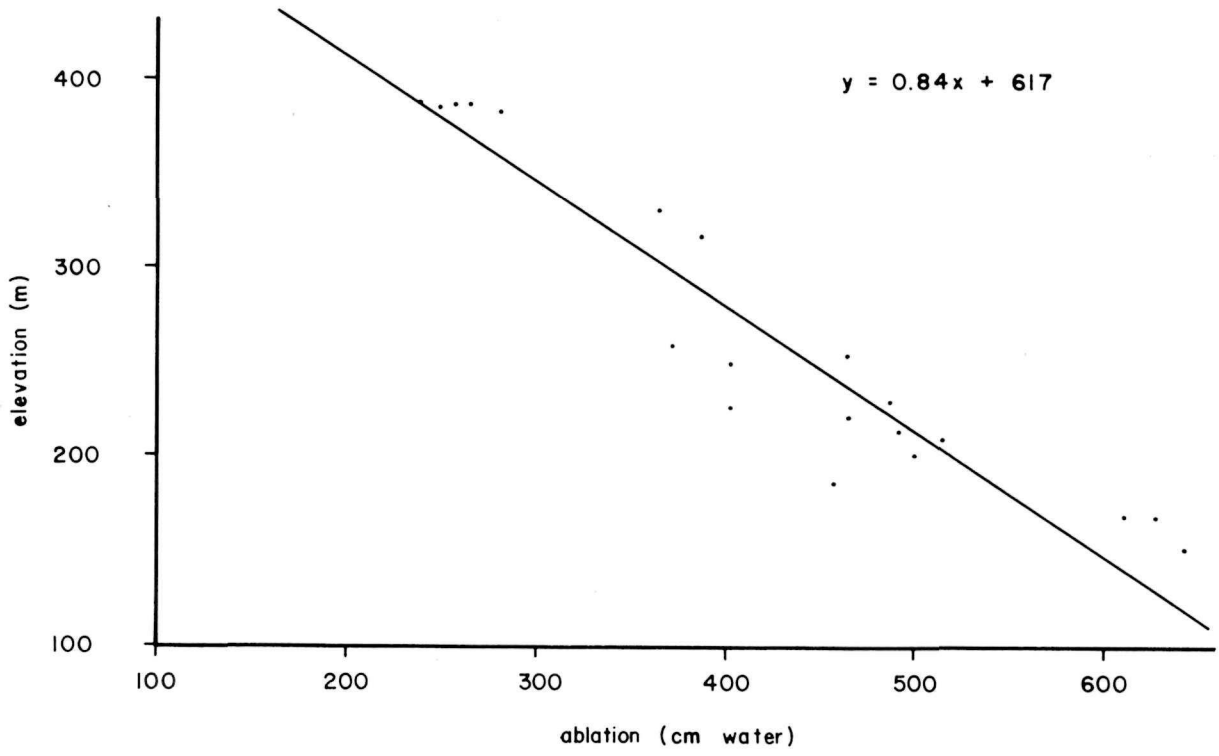

Figure 9. Plot of ablation vs. elevation on Burroughs Glacier, 1973.

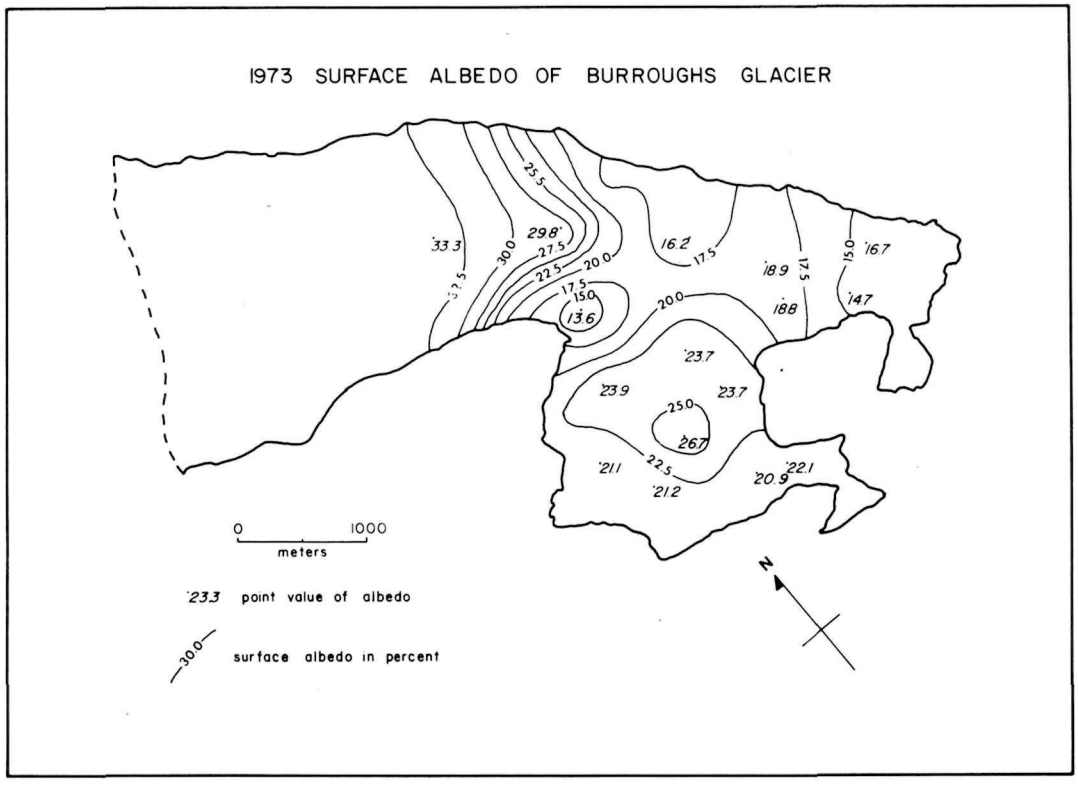

Fig. 10

recorded by suspending the pyronometer 2 m above the ice surface in a level inverted position. The measured albedo ranged from 13 percent near the terminus to 33 percent on the higher part of the glacier. The variances in albedo are presumably due to changes in the dirt content and color of the glacier surface.

INFLOW

Inflow of meltwater into a glacier can be determined by calculating the heat-energy balance at the glacier surface. This is usually a formidable task because there are several sources of heat energy that contribute to the surface melting process. There is heat energy in the form of radiation from the sun and sky, and sensible heat from conduction and convection through the overlying air mass. Condensation of water vapor on the ice surface and conduction from warmer ice below the surface are also sources of heat energy. Another source is rain, which falls on the glacier during the summer.

Heat energy is also expended from the glacier surface in a variety of ways. It can be conducted downward into the glacier or withdrawn by sublimation of ice, snow, or water. It is also lost from the surface by the emission of long-wave radiation, especially at night.

Most energy balance studies on glaciers are based on records from one or possibly two micrometeorological stations on the ice. The great complexity of spacial variations (wind, temperature, humidity, etc.) on a glacier surface, however, can rarely be treated on this basis. For example, heat-energy from rain alone will vary areally with intensity, duration, and temperature of the rainfall.

In this report, an approach is taken which simplifies the calculation of the heat-energy balance and melt on a glacier surface. First, each component of heat-energy balance is determined for a single point on the glacier surface during a nearly cloudless four-day period. Once it is established that global radiation is the most dominent source of heat energy for melting, calculations are made to estimate the melt at numerous other points on the glacier based on global radiation receipts alone.

Instrumentation

To record the parameters of the heat balance equation at a single site, a micrometeorological station was maintained on Burroughs Glacier from 0000 h, August 14 to 2400 h, August 17, 1973. The station was located about 200 m from the glacier terminus (Fig. 2). The surface of the glacier at the site of the station sloped southeast at about 15^{o}. The weather during the period of observation was characterized by clear skies, no rain, and above average temperatures. Some cloudiness and haze, however, did occur during the afternoon of August 14. A summary of the meteorological conditions during this period is presented in Table 1.

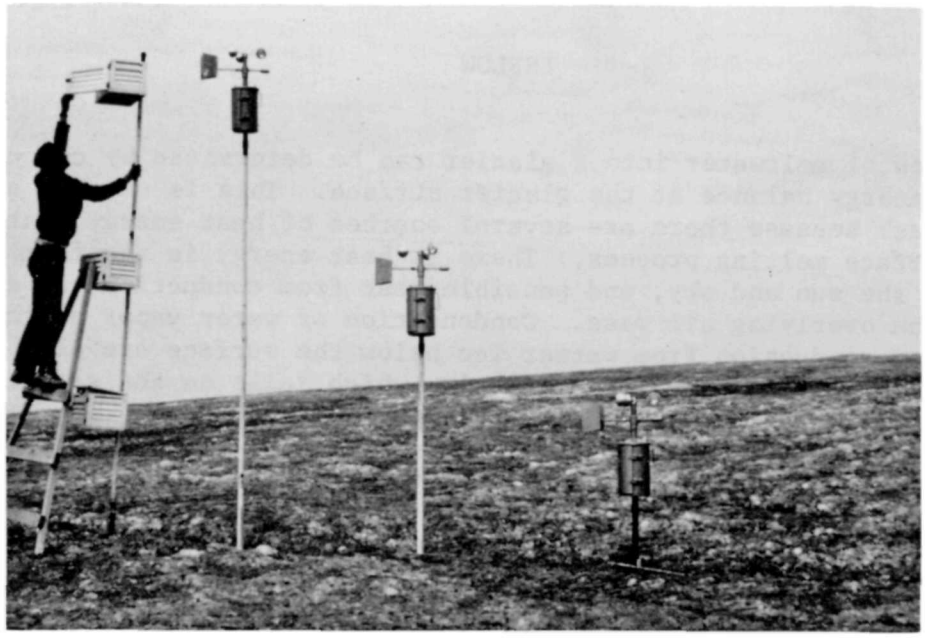

Figure 11. Micrometeorological station with wind recorders and weather screens 1.0, 2.0, and 3.5 m above the glacier surface.

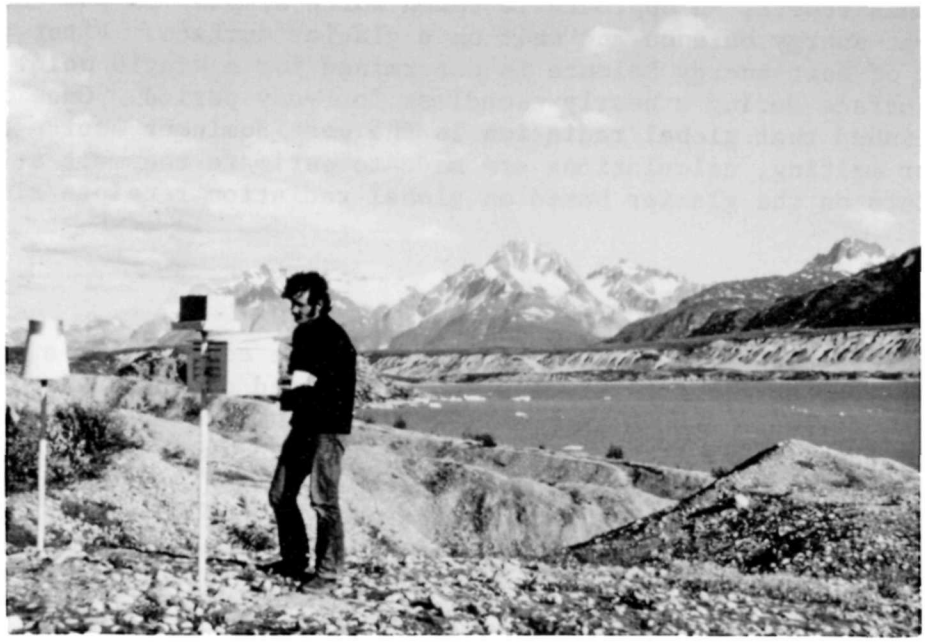

Figure 12. Camp meteorological station with Belfort pyheliograph and rain gage.

TABLE I

SUMMARY OF METEOROLOGICAL CONDITIONS DURING
THE PERIOD AUGUST 14-17, 1973
BURROUGHS GLACIER, ALASKA

	August 14	August 15	August 16	August 17
Temperature (C^{o}) max/min	13.4/6.2	15.7/5/6	17.2/9.0	16.2/9.0
Relative humidity (%) max/min	90/57	96/44	61/42	57/46
Precipitation (mm)	0.0	0.0	0.0	0.0
Wind velocity (m/s)	1.0-2.0 S.W.	0.5-2.5 S.W.	0.5-2.0 S.W.	0.5-2.5 S.W.
Cloud cover (%)	10	0	0	0
Global radiation (ly/day)	473.4	537.6	515.4	545.4

Wind speed, temperature and relative humidity at the micromet station (Fig. 11) were recorded continuously at three levels (1, 2, 3.5m) above the glacier surface. Model 1482 Lambrecht wind recorders were used to measure the wind velocity and direction. The air temperature and relative humidity were recorded with Casello model 257 hygrothermographs set within Stevenson type screens. Each hygrothermograph was calibrated before use, and was regularly checked against numerous psychrometic readings to test for radiative heating by the weather screens. During the entire period of observation no significant radiative heating was detected, probably because of the strong ventilating effect of the wind, which persisted during that time.

Short-wave radiation receipts were recorded with a Belfort pyheliograph model 5-3850. The instrument, maintained at the base camp approximately 2 km from the micromet station (Fig. 12), was mounted on a horizontal platform 1.7 meters above the ground surface. An Epply pyranometer model 8-48 and a Leads and Northrop potentiometer model 8696 were used to calibrate the pyheliograph. Precipitation was also recorded at the base camp with a standard 20-cm-diameter rain gage. A list of all the meteorological instruments may be found in Appendix A. Meteorological data and computational data from the micromet station are also included in the Appendix.

The Heat Energy Balance

In general, the heat-energy balance at the melting ice surface may be written as:

$$Q_{rs} \pm Q_{rl} \pm Q_s \pm Q_l \pm Q_i \pm Q_p = Q_{ml},$$

where Q_{rs} is the net shortwave radiation flux, Q_{rl} is the net long-wave radiation flux, Q_s is the heat transfer by convection between the surface and the atmosphere, Q_l is the heat transfer by evaporation or condensation, Q_i is the heat transfer by conduction from the surface to the interior of the glacier or from the interior to the surface, Q_p is the heat transfer by precipitation, and Q_{ml} is the total heat used in melting. During the period 14-17 August, each component of the heat energy balance equation was evaluated on an hourly basis.

Net Short-Wave Radiation. The short-wave radiation balance (Q_{rs}) on a surface is the algebraic sum of incoming global radiation and reflected short-wave radiation. An expression for this relationship is as follows:

$$Q_{rs} = I_g - I_r,$$

where I_g is the global radiation from the sun and sky, and I_r the reflected short-wave radiation. Global radiation (I_g) is the sum of direct solar radiation (I_d) from the sun and diffuse radiation (D) from the sky:

$$I_g = I_d + D.$$

Following Garnier and Ohmura (1968), the daily total of direct solar radiation falling upon a slope may be written:

$$I_d = {}^{I_o}/_{r^2} \int_{H_1}^{H_2} p^m \cos(x\Lambda s)\, dH, \qquad (1)$$

where I_d is in langleys, I_o is the solar constant taken as 2.0 cal cm^{-2} min^{-1}, r is the radius vector of the earth's orbit, H_1 and H_2 are the hour angles when the sun shines on the slope for the first and last times each day, p is the mean-zenith-path transmissivity, m is the optical air mass, and H is the hour angle measured from solar noon, positive after noon. The expression cos (xΛs) is the cosine of the angle of incidence of the sun's rays on a slope and is equal to $(-\sin\phi \cos H \cos A \sin\theta) - \sin H \sin A \sin C + \cos\phi \cos H \cos\theta)\cos\delta + (\cos\phi \cos A \sin\Theta + \sin\phi \cos\Theta) \sin\delta$, where ϕ is latitude, A the azimuth of the slope, Θ is the angle of the slope, and δ is the declination of the sun. For computational purposes, it is convenient to write cos (xΛs) as $(C_1 \sin H + C_2 \cos H + C_3)$, where $C_1 = \sin A \sin\Theta \cos\delta$, $C_2 = (\cos\phi \cos\Theta - \sin\phi \cos A \sin\Theta) \cos\delta$, and $C_3 = (\sin\phi \cos\Theta + \cos\phi \cos A \sin\Theta) \sin\delta$. Alternatively, cos (xΛs) may be expressed as a function of hour angle H such that:

$$f(H) = C_4 \cos (H = \Psi) + C_3, \quad (2)$$

where $C_4 = (C^2 + C_2{}^2)^{\frac{1}{2}}$ and $\Psi = \arctan (C_1/C_2)$. Expression (2) is convenient because in the absence of shadow, the sun's rays are incident on the slope when f(H) is positive.

The diffuse radiation (D) falling upon a sloping surface can be estimated by the formula:

$$D = D_o \cos^2 (\Theta/2),$$

where Θ is the slope angle and D_o is the diffuse radiation falling on a horizontal surface. Following Williams, Barry, and Andrews (1972), the daily total of diffuse radiation falling on a horizontal surface may be calculated by a simple clear-sky approximation:

$$D_o = o.5 (1 - A_w - A_o) I_t - I_h), \quad (3)$$

where A_w is the proportion of radiation absorbed by water vapor in the atmosphere (7%), A_o is the proportion absorbed by ozone (2%), I_t is the extraterrestrial radiation:

$$I_o/r^2 \int p^m \cos Z_s \, dH,$$

and I_h is the direct radiation on a horizontal plane at the surface:

$$I_o/r^2 \int p^m \cos Z_s \, dH.$$

Rewritten, (3) can be expressed as:

$$D_o = 0.5 \, I_o/r^2 \int_{H_1}^{H_2} (0.91-p^m) \cos Z_s \, dH. \quad (4)$$

The optical air mass M in (1) and (4) can be written as a function of time H by using a secant approximation:

$$m = \sec Z_s = 1/\cos Z_s, \quad (5)$$

where Z_s is the zenith angle of the sun. Since m is determined from a horizontal surface, cos Z_s is equal to cos δx cos ϕx cos H + sin δx sin ϕ. Estimating m by (5), however, usually underestimates solar radiation, especially when $Z_s > 70^o$. This is because the earth's atmosphere is curved and refracts radiation at low sun altitudes (Halliner and Martin, 1957; de Brichambaut, 1963; Kondratyev, 1969). Garnier and Ohmura (1968), however, demonstrate that the degree of error varies with latitude and time of year. They suggest that the potential error for the month of August at 59^o N latitude is not more than 10 percent of the daily total. Therefore, the secant approximation appears valid.

Expressions (1) and (4) are not mathematically integrable, but their solutions are possible by summation for small interval of H:

$$I_d = {}^{I_o}/_{r^2} \sum_{K=1}^{N} p^{mk} f(H_k) \quad \Delta H, \; f(H)>0$$

$$D_o = 0.5 \; {}^{I_o}/_{r^2} \sum_{K=1}^{N} (0.91-p^{mk}) \cos Z_s \; \Delta H.$$

It was found during the course of this study that an interval of 30 minutes for H gave sufficient accuracy. The only element not yet determined in the equations is the atmospheric transmissivity (p). This value changes from day to day but can be estimated by comparing the computed daily global radiation falling on a horizontal surface with the global radiation recorded with the pyheliograph at the base camp. The values for atmospheric transmissivities calculated for the four days were found to be 0.51, 0.67, 0.64 and 0.71.

The amount of radiation reflected (I_r) from the glacier surface can be expressed as the product of the surface albedo (α) and the flux of global radiation (I_g) incident to the surface:

$$I_r = \alpha I_g.$$

The albedo of a glacier surface, however, does not stay strictly constant. It changes with the angle of solar inclination and with the wetness and roughness of the ice surface (Lister and Taylor, 1961). Keeler (1964) found a diurnal variation of ± 10 percent for the albedo of Sverdrup Glacier in the Northwest Territories and noted that the albedo generally increases with decreasing angle of solar inclination. Andrews (1964), on the other hand, found that the surface albedo of White Glacier in the Canadian Arctic Archipelago decreases with decreasing angle of solar inclination.

In this study, no detailed investigation was made of the daily variation in albedo at the site of the micrometeorlogical station. Therefore, a constant albedo of 22 percent (Fig. 11) was assumed to calculate the reflected radiation.

Net Long-Wave Radiation. The net long-wave radiation (Q_{rl}) is the algebraic sum of the long-wave radiation from the atmosphere (R_a) and the outgoing long-wave radiation from the ice surface (R_s):

$$Q_{rs} = R_a - R_s.$$

Instruments for measuring net long-wave radiation ($R_a - R_s$) were not available for this study: therefore, it was approximated by an empirical formula. The expression used in this approximation was developed by Hoinkes and Untersteiner (1952) and is of the form:

$$R_a - R_s = R_o\left(1-K\left(\frac{C^2}{10}\right)\right),$$

where R_a is the long-wave radiation from the atmosphere, R_s is the outgoing long-wave radiation from the ice surface, R_o is the effective radiation under clear skies, and C is the cloudiness in tenths. The value K is a constant which varies with the height and type of clouds. Andrews (1964) suggested that K is equal to 0.2 for cirrus clouds, 0.6 for medium-height clouds, and 1.2 for low clouds.

The effective radiation under clear skies (R_o) was not recorded in this study. However, other studies have shown that under clear skies, R_o can range from 0.085 (Ambach, 1960) to 0.16 cal $cm^{-2}min^{-1}$ (Sverdrup, 1936). The value of 0.12 was adopted for this study as this was the value recorded under cloudless sky for August at Pavlovsk, U.S.S.R. which lies almost at the same latitude as Burroughs Glacier (Kondratyev, 1969).

Transfer of Sensible and Latent Heat. The equation for the calculation of sensible heat (Q_s) may be written:

$$Q_s = C_p A \frac{dT}{dz} t$$

where C_p is the specific heat of air at constant pressure (0.24 cal/gm°C), A is the exchange coefficient (gm/cm sec), dT/dz is the vertical gradient of potential temperature (taken as observed °C/cm) and t is the time interval in seconds.

The latent heat (Q_l) may be expressed in similar fashion by:

$$Q_l = L A \frac{0.623}{p} \frac{de}{dz} t,$$

where L is the latent heat of condensation (600cal/gm), p is the atmospheric pressure (mmHg), and de/dz is the vertical gradient of vapor pressure (mmHg/cm).

Before Q_a and Q_l can be evaluated, however, the exchange coefficient A must be determined from observed quantities. This is done by expressing the variation of wind (μ), temperature (T), and vapor pressure (e) with height above the surface in mathematical form. Wallen (1948) and Andrews (1964) both found that the vertical variation of these elements under stable atmospheric conditions is best expressed by the power law of the type:

$$a - a_1 (z/z_1)^{\frac{1}{n}},$$

where a and a_1 are the elements (wind, temperature, vapor pressure) recorded at height z and z_1 above the surface, and n is the power law index of the element which varies according to conditions under which the study is made.

Havens and others (1965) and Grainger and Lister (1966), however, suggest that the wind profile under neutral or near-neutral conditions is best expressed by a logarithmic relationship of the form:

$$\mu_z = C \log \left(\frac{z-z_o}{z_o}\right),$$

where μ_z is the wind at height z, C is a constant, and z_o is a surface roughness parameter. Other researchers (Derikx, 1973) have also suggested a logarithmic-plus-linear profile to express the variation of wind speed above the surface.

Analysis of the temperature, vapor pressure, and wind speed recorded at the three levels of the micrometeorological station suggests that the power-law formula provides the best approximation of the wind, temperature, and vapor-pressure profiles, especially during periods of extreme stability. From this formula, values for the power-law indices for the wind (N_u), temperature (N_T) and vapor pressure (N_e) were calculated for each hourly interval from August 14 to 17. The exchange coefficient (A) was then determined for height Z by the general expression (Havens, 1964):

$$A = K\, u_z\, A\left(\frac{N_T - 1}{N_T} - \frac{1}{N_u}\right),$$

where k is a constant equal to 1.78×10^{-4}. This value was calculated by Wallen (1948) for Karso glacier and is probably representative of the condition on Burroughs Glacier.

Heat Conducted into the Ice. The heat flow per unit time through the ice can be expressed as:

$$Q_i = p\, C_i \int_{Z_1}^{Z_2} \Delta T\,(Z)\, dz,$$

where p is the density of the ice, C_i is the specific heat of ice, and ΔT is the change in temperature over depth Z. The direction of heat flow depends on whether temperature increases or decreases with depth. Since Burroughs Glacier is assumed to be at the pressure melting point throughout, heat-flow through the ice should be negligible.

Heat from Rain. The heat supplied by rain to the ice surface can be calculated using the expression:

$$Q_p = C_w\, P\, (T_p - T_s),$$

where C_w is the specific heat of water, P the precipitation in g cm^{-2}, and T_p and T_s are the temperature of the rain and the surface. However, since there was no precipitation during the period August 14 to 17, this term was not considered in the heat-energy balance.

Discussion of Errors. There are several possible sources of error in calculating the heat-balance equation. One lies in assuming no departure from stability exhibited by the atmosphere overlying the glacier surface. If instability were to occur, the power-law formulation for the expression of the variation of wind speed, temperature, and vapor pressure would not be valid. The steep temperature gradients recorded at the micromet station from August 14 to 17, however, suggest that the atmosphere was quite stable during that period.

Another source of error lies in choosing a value for the constant, k, in the calculation of the exchange coefficient (A). Andrews (1964), for example, found that k is affected by wind and temperature, and suggests that it can vary from location to location. A source of error also lies in the accuracy of the temperature and humidity data. The available instruments together with the weather screens were probably not perfectly suited to the task of measuring these elements under actual field conditions. It is hoped, however, that the careful calibration of the instruments and constant field checking of the recorded values has minimized this source of error.

Error may also be introduced in the measurement of global radiation and in the calculation of the radiant heat flux. The technique for calculating direct radiation and diffuse radiation incident upon a slope assumes that the measured global radiation receipts are accurate. This assumption appears valid because the measured daily global radiation for August 14 to 17 compares favorably with published values of global radiation measured under clear skies at the same latitude and the same time of year (Kondratyev, 1969).

The transmissibility of the atmosphere is taken to be constant throughout the day; obviously this may not always be true, and any variations could lead to error. A constant albedo for the ice surface is also assumed, yet as already indicated, studies have shown that it can vary with weather conditions and the angle of solar incidence. The technique for estimating the net flux of long-wave radiation is also subject to error in that it is based on qualitative measurements of cloud cover and altitude of the cloud base. These potential errors are about impossible to estimate. It must be emphasized, however, that the main purpose of the heat-balance study was not to precisely calculate each component of the heat-balance equation, but to obtain a realistic estimate of the relative significance of each component in the melting process.

The Heat-Balance as a Whole. The algebraic sum of all the heat-energy sources is the residual heat (Q_{ml}) available for melting. From August 14 to 17, Q_{ml} ranged from 259 to 565 langleys day^{-1}. The hourly values of each source are diagrammed in Figured 13, while the daily totals of each components are listed in Table 2, together with their relative significance in percent. It can be seen from the data that global radiation (I_g) was the most important heat source for melting. On August 15, for example, global radiation contributed well over half of the total heat energy. Heat balance studies made on nearby Casement Glacier during clear sunny days (Peterson, 1970) have shown similar results.

Comparison Between Surface Lowering and Calculated Ablation. A certain indication as to the accuracy of the heat-balance data can be obtained by comparing the daily calculated melt with the observed melt. The calculated melt, in cm of water per day, is obtained by dividing the heat of fusion of ice (80 g cal cm^{-2}) into the algebraic sum of the heat energy components. The observed daily melt, on the other hand, is determined by noting the amount of surface lowering of the ice at the micromet station and calculating the water equivalent. This was done every 24 hours during the four day period.

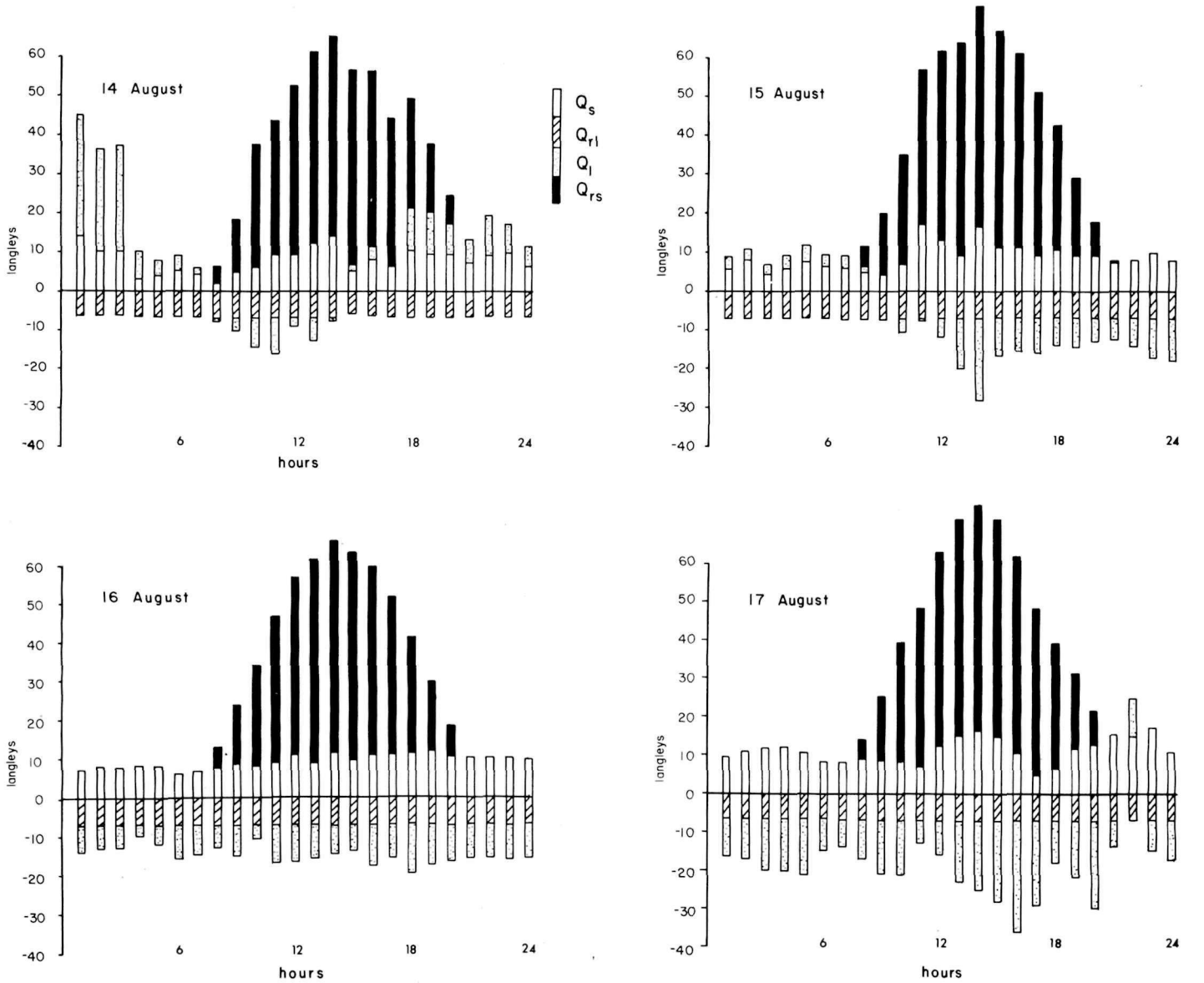

Figure 13. Relative importance of short-wave (Q_{rs}) and long-wave (Q_{rl}) radiation, latent heat (Q_l), and sensible heat (Q_s) as heat sources and sinks on Burroughs Glacier from August 14 through 17, 1973.

It can be seen from Table 2 that for the period August 14 through 17, the agreement between calculated and observed melt is good on some days, and poor on other days. For example, on August 15 and 16, measured and theoretical values match very well. On August 14 and 17, however, there is a significant discrepancy between the two values. Such discrepancies are not unusual, and have been noted in other heat balance studies (Keeler, 1964; Andrews, 1964; Havens and others, 1965; Wendler and Weller, 1974). They are usually attributed to changes in the surface density caused by radiation melting along ice crystal boundaries. Most major discrepancies occur after a sudden change from low-radiation heating to relatively high-radiation heating. Such seems to be the case for August 14.

TABLE 2

SUMMARY OF HEAT BALANCE COMPUTATIONS

Day	Q_s		Q_l		$I_g - I_r$		$R_a - R_s$		Q_m	Melt	
										calc.	meas.
	(ly)	(%)	(ly)	(%)	(ly)	(%)	(ly)	(%)	(ly)	(cm)	(cm)
August 14:	184	25	124	18	414	57	-167	-100	565	7.06	2.5
August 15:	205	31	-99	-36	464	69	-171	-64	399	4.98	4.6
August 16:	218	33	-193	-46	445	67	-162	-54	308	3.85	3.8
August 17:	264	36	-307	-65	470	64	-168	-35	259	3.24	4.8
Total	871		-465		1793		-668		1531	19.13	15.1

Melt Over the Entire Glacier Surface

It has already been demonstrated that, during the period August 14 through 17, global radiation was the dominant heat source for melting. A closer look at the data presented in Figure 13 would also show that, if the heat sinks were subtracted from the heat sources, global radiation would account for almost all of the daily melt on the glacier. Based on this observation, it should be possible to estimate the melt over the entire glacier during the four days by calculating the theoretical net global radiation received at numerous points on the ice surface.

Surface Geometry of the Glacier - Figure 14 shows the location of 1176 points on Burroughs Glacier where calculations were made of the surface slope and net global radiation. The points are arranged in a regular north-south, east-west matrix and have a spacing interval of 100m. To fix each point in space, elevations for the points were determined using the 1970 topographic map of Burroughs Glacier shown in Figure 2. In addition, the albedo of the ice at each point was obtained from the albedo map in Figure 11.

The slope and azimuth of slope calculated for each point are shown in Figures 15 and 16. The values were determined by statistically fitting, with the aid of a digital computer, a linear regression plane through every set of nine points in a three by three matrix. In cases where a point lay along the margin of the glacier, the slope and slope azimuth were approximated by fitting a plane to the point in question and any two or more adjacent points on the ice. The calculated slopes on the glacier ranged from 0 to 23 degrees with over 70 percent of the surface sloping 5 degrees or less. With respect to azimuth of slope, approximately 17 percent of the glacier surface had a northeasterly exposure, 62 percent a southeasterly exposure, 19 percent a southwesterly exposure, and 2 percent a northwesterly exposure.

Undoubtedly, there have been some changes in the surface geometry of Burroughs Glacier from 1970 to 1973, especially near the ice margin. The slope and azimuth of slope over most of the glacier, however, have probably not changed very significantly during the three years. Therefore, both the slope and slope azimuth values in Figures 15 and 16 are useful for calculating the net global radiation received by the glacier during the period August 14 through 17, 1973.

Areal Variability of Global Radiation - The areal variability of incoming global radiation on Burroughs Glacier during the period August 14 through 17 is shown in Figure 17. The values for the four-day period were obtained by calculating the theoretical flux of incoming global radiation for each point shown in Figure 14. It is evident from the data that there is some surface zoning of global radiation on the glacier, and, as one would expect, southerly exposures receive more radiation than northerly exposures. The flux of incoming global radiation for the four days ranged from just under 2000 cal cm^{-2} to a little over 2200 cal cm^{-2}.

Figure 18 shows the areal variability of melt on Burroughs Glacier during the same four-day period. The melt was calculated from theoretical values of net global radiation calculated for each point in Figure 14. The range of melt in centimeters of water for the four days ranged from 16.7 near the glacier divide to just over 26 cm near the glacier terminus. The total volume of melt on the glacier surface was approximately 24.24 $10^5 m^3$ of water.

The curves in Figure 19 show the rate of melt on Burroughs Glacier from August 14 through 17. The curves were derived by calculating the flux of net global radiation received by the glacier every 30 minutes. The curves clearly show that melt from global radiation begins each day at approximately 0730h and reaches a maximum at about 1430h. The total daily melt from global radiation is printed under each curve and ranges from $5.26 \times 10^5 m^3$ to $6.52 \times 10^5 m^3$.

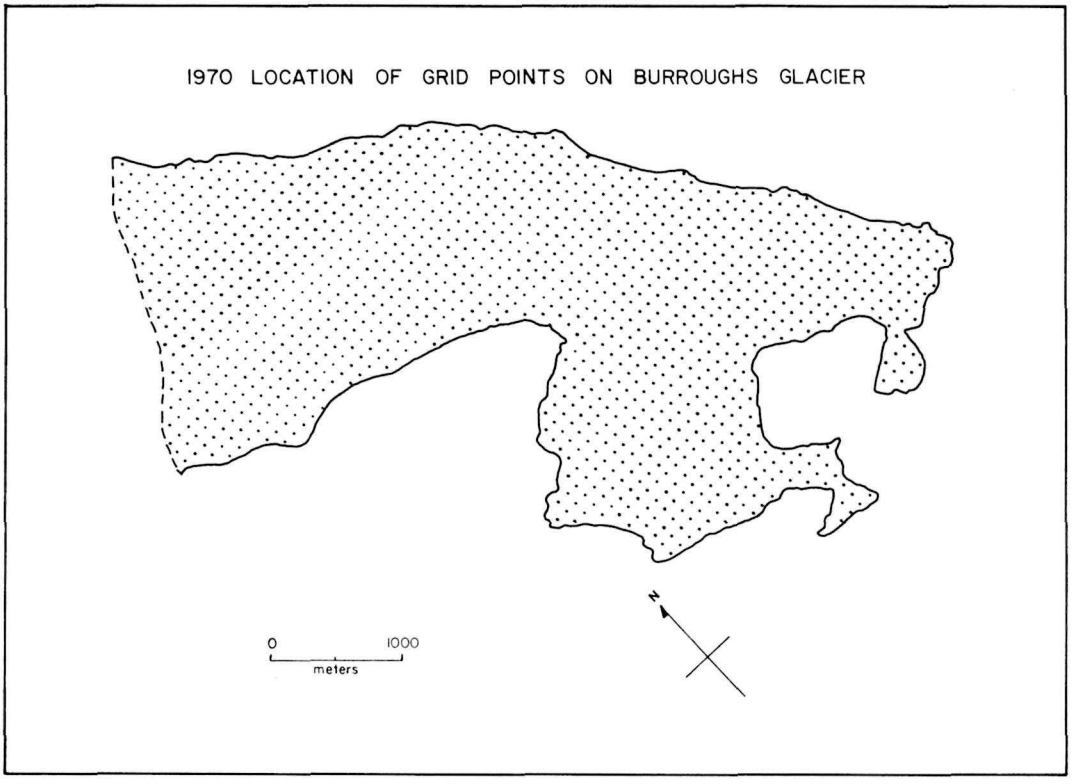
1970 LOCATION OF GRID POINTS ON BURROUGHS GLACIER
0
1000
meters
N

Fig. 14

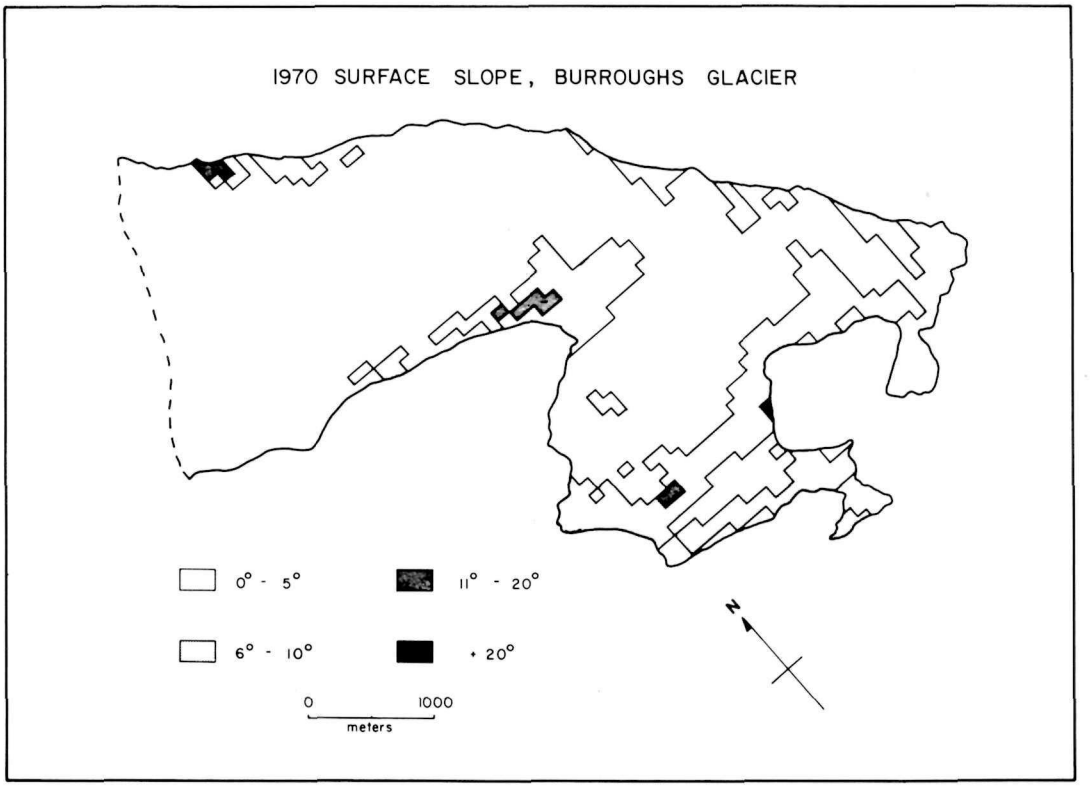
1970 SURFACE SLOPE, BURROUGHS GLACIER
0° - 5°
11° - 20°
6° - 10°
+ 20°
0
1000
meters
N

Fig. 15

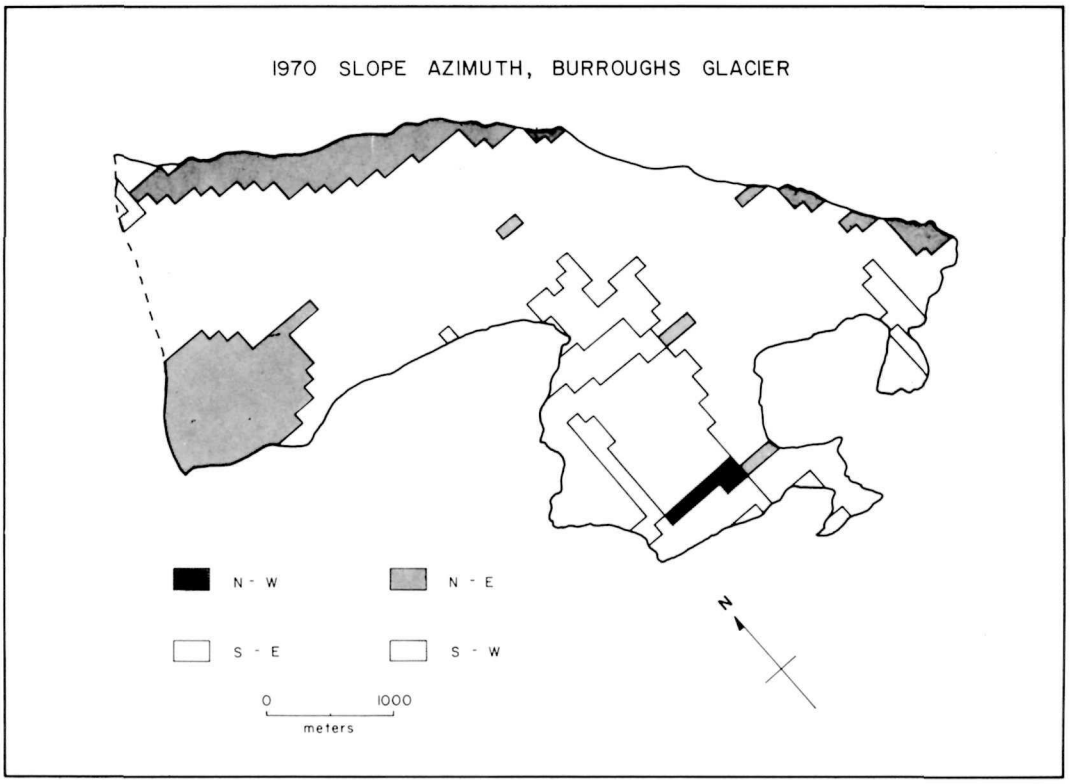
1970 SLOPE AZIMUTH, BURROUGHS GLACIER
N - W
N - E
S - E
S - W
0
1000
meters
N

Fig. 16

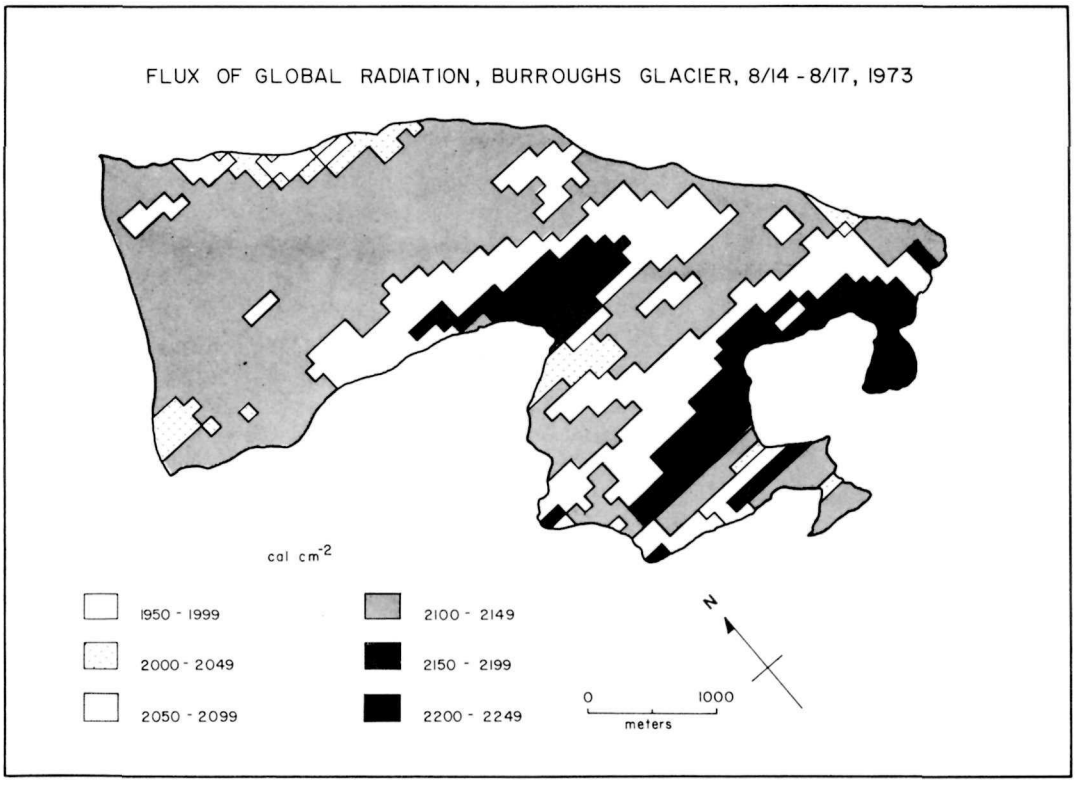
FLUX OF GLOBAL RADIATION, BURROUGHS GLACIER, 8/14 - 8/17, 1973
cal cm^{-2}
1950 - 1999
2000 - 2049
2050 - 2099
2100 - 2149
2150 - 2199
2200 - 2249
0
1000
meters
N

Fig. 17

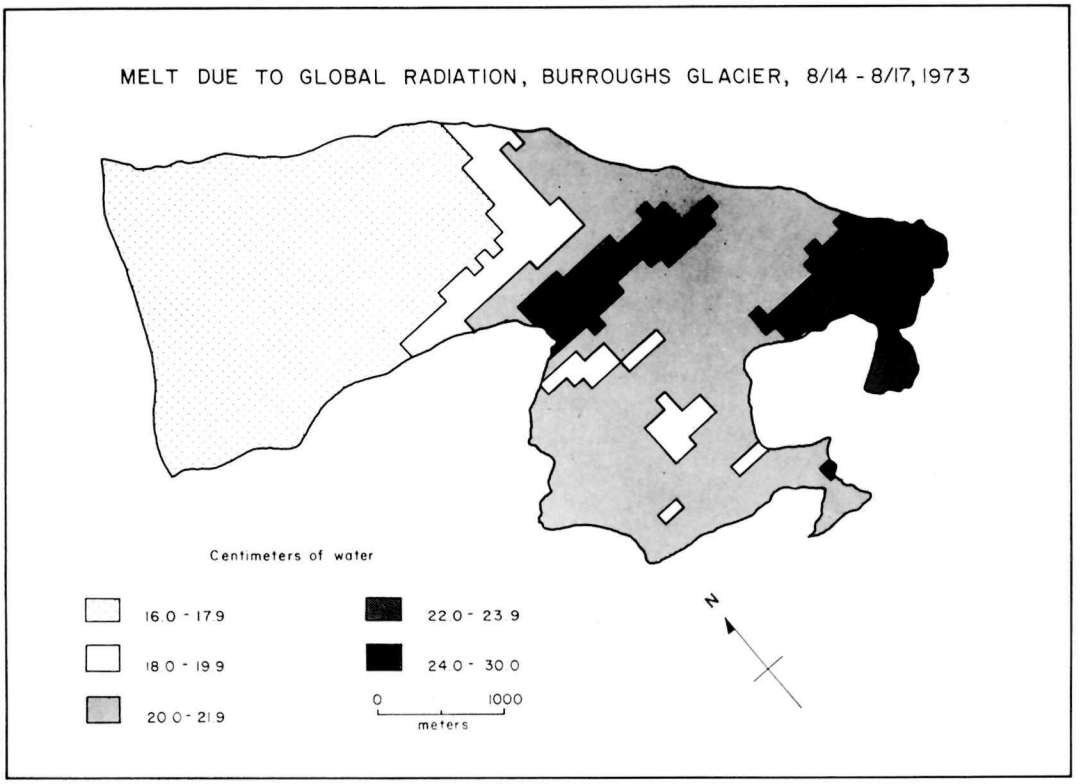

Fig. 18

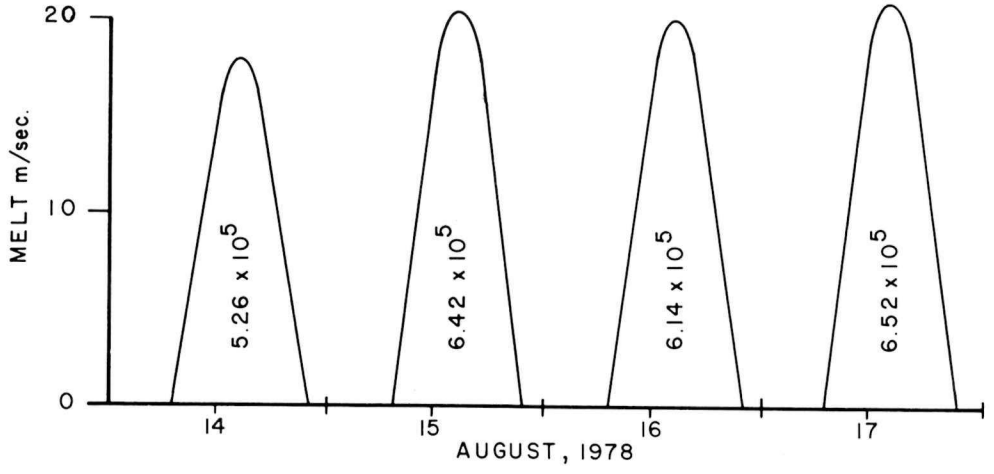

Figure 19. Rate of melt on Burroughs Glacier from short-wave radiation during the period August 14 through 17, 1973.

At low sun angles, some shadows are cast on the glacier from the surrounding hills. Undoubtedly, they must effect the rate and total amount of melt on the glacier surface. The net effect of the shadows, however, is probably minimal, because at low sun angles, the flux of global radiation on the glacier is very small. Also, since the exposure of the glacier is mostly east-west, most of the shadows are limited to just after sunrise and just before sunset.

OUTFLOW

The location of each stream draining meltwater from Burroughs Glacier is shown in Figure 20. The largest of the streams, Burroughs River, flows from the eastern end of the glacier and discharges into Wachusett Inlet. In places its channel is as much as 12 m wide. Gull Creek, on the other hand, is a somewhat smaller stream which emerges from the southwestern edge of the glacier and flows into Wachusett Inlet. The smallest stream draining the glacier is Bob Creek. It is only a meter or two wide and flows from an extension of ice on the southeastern side of the glacier and joins the Burroughs River about 1 km downstream from the ice edge.

Also shown in Figure 20 are the locations of gaging stations set up during the summer of 1973 to record discharge in the three streams draining the glacier. The station on Bob Creek (Fig. 21) is located approximately 0.5 km downstream from the glacier margin and at a point where the stream is confined to a bedrock channel. The station on Gull Creek (Fig. 22) is about 0.6 km from the glacier and is also situated at a point where the stream channel is underlain entirely by bedrock. The Burroughs River gaging station (Fig. 23) is about 0.5 km downstream from the ice edge. Unlike the other locations, the stream channel at the station is underlain by both bedrock and coarse gravel.

Each gaging station, constructed of wood and plastic pipe, was equipped with a Stevens water-level recorder and eight-day mechanical clock (Fig. 24). The wood was used for housing the recorders, whereas the pipe served for the stilling wells. Rating curves for the stations (Fig. 25) were constructed by measuring stream discharge directly with a Gurley current meter and pigmy meter. To simplify conversion of stream stage to discharge, each rating curve was approximated by a parabolic equation of the form

$$Q_t = C(G_t - z)^N,$$

where Q is discharge, G is stage at time t, C and N are constants, and a is the stage at 0 discharge.

Outflow from Burroughs Glacier

The discharge hydrographs for Bob Creek, Bull Creek, and Burroughs River from August 13 to 19, 1973 are shown in Figure 26. It is evident from the curves that runoff from the glacier follows a general diurnal pattern, with peak discharge occurring each day around 1700 h to 1900 h. The only exception is on August 13 when discharge in the streams was unusually high and sporadic due to heavy rain (2.2 cm day^{-1}) falling within the glacier basin. The broken line appearing under each record is a runoff recession curve associated with the rainstorm. The

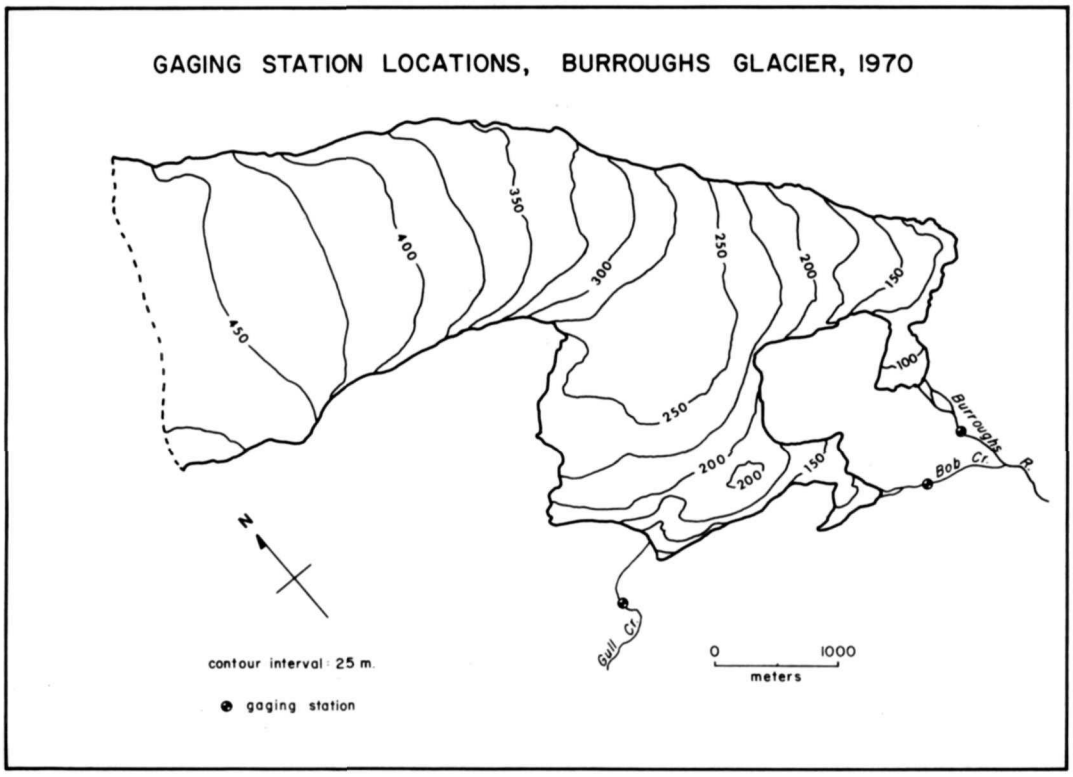

Fig. 20

Figure 21. Gaging station on Bob Creek.

Figure 22. Gaging station on Gull Creek.

Figure 23. Gaging station on Burroughs River.
(station located in lower left of photograph)

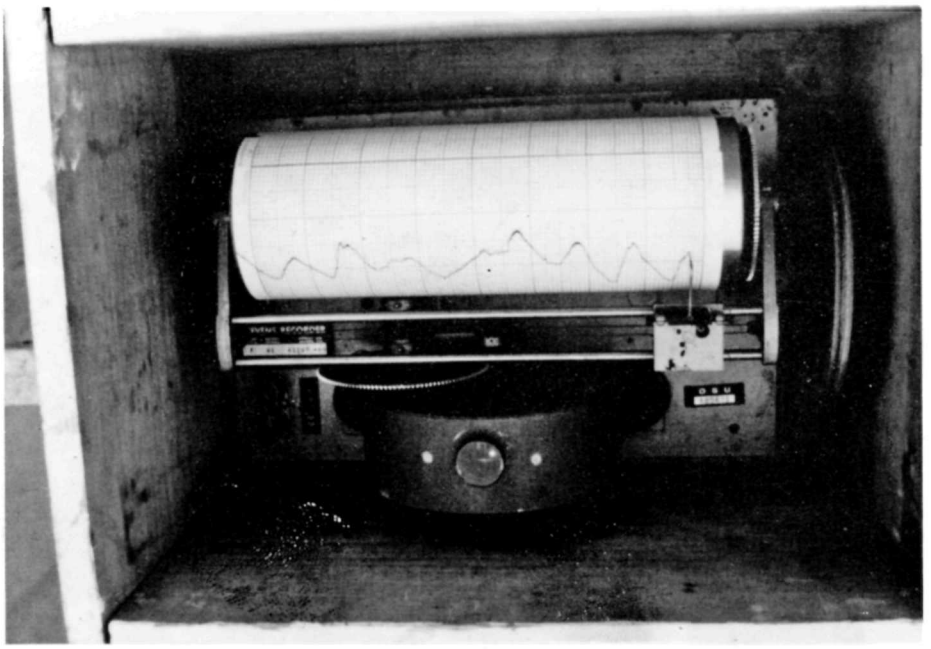

Figure 24. Inside of gaging station housing showing Stevens water-level recorder, eight day clock, and stage hydrograph.

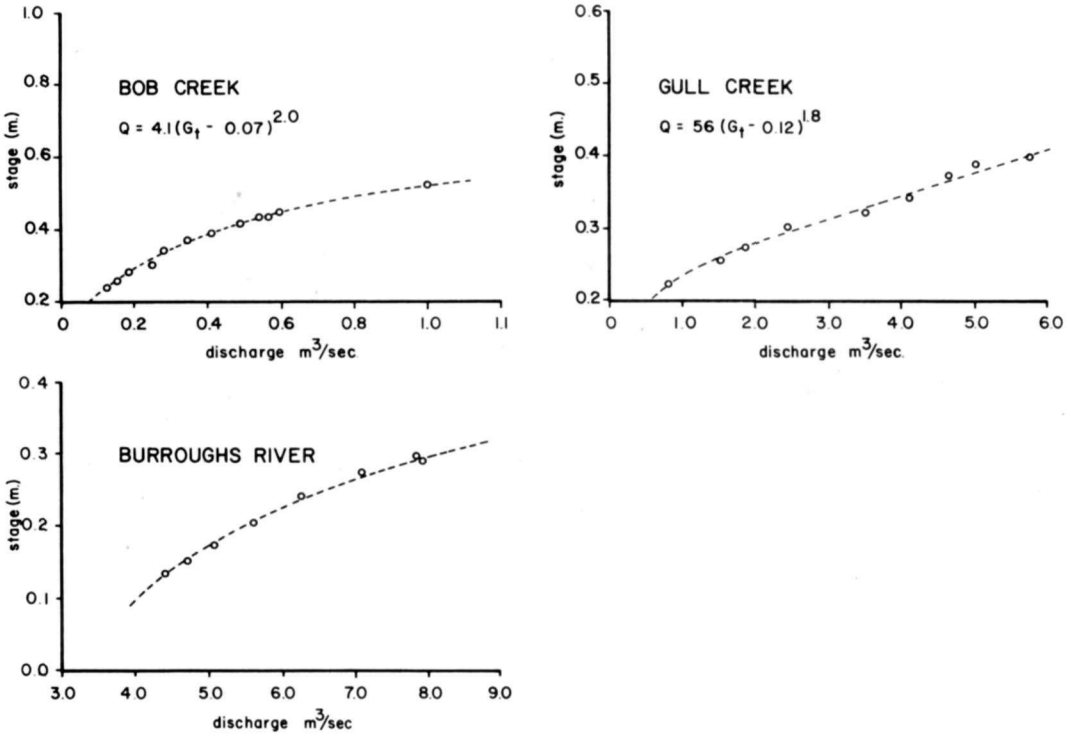

Figure 25. Rating curves for Bob Creek, Gull Creek and Burroughs River.

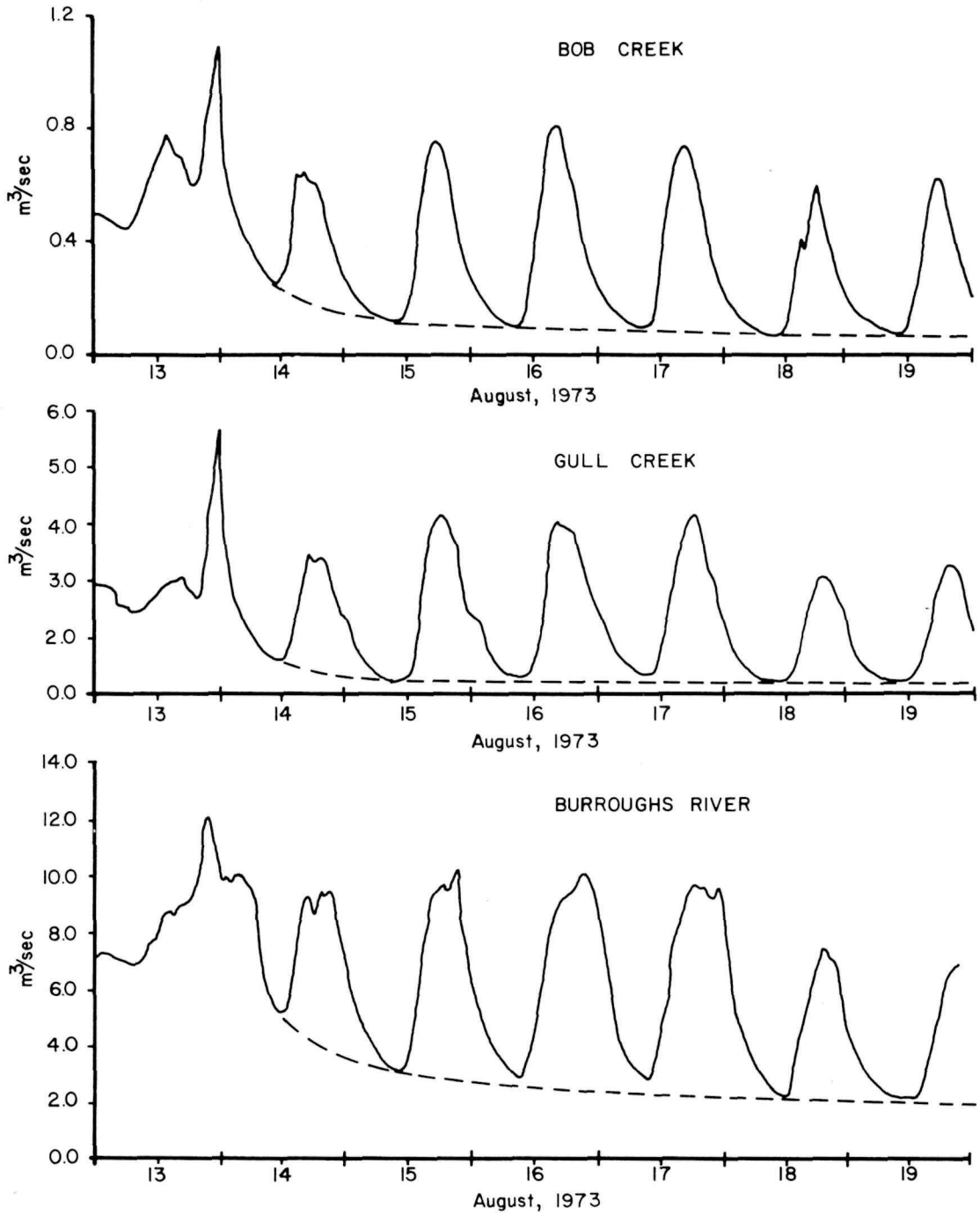

Figure 26. Discharge records for Bob Creek, Gull Creek, and Burroughs River from August 13 through 19, 1973.

curves were approximated by fitting a line through the diurnal throughs that developed after cessation of precipitation. Both the recession curves and recorded discharges clearly show that outflow from the glacier during the period August 13 to 19 was a combination of both meltwater runoff and delayed storm runoff.

The recorded discharge in each stream minus the storm runoff from August 14 to 18 is shown in Figure 27. The records reveal a series of single and multi-peaked hydrographs each consisting of two parts: a rising segment and recession segment. In most cases the rising segment tends to be convex upwards, rising rapidly at first and then, more gradually towards the end of the rise. The recession segment, on the otherhand, falls with gradually decreasing slope, thus indicating that meltwater runoff from the glacier is greatly dependent on meltwater storage within the glacier. Table 3 lists the daily outflow of meltwater from the glacier and shows that approximately 60 percent of the total melt flows into Burroughs River, 36 percent into Gull Creek, and 4 percent into Bob Creek.

TABLE 3

DAILY DISCHARGE OF MELTWATER
FROM BURROUGHS GLACIER
August 14-18, 1973
($\times 10^5 m^3$)

	August 14	August 15	August 16	August 17	Total	
Bob Creek	0.15	0.19	0.23	0.22	0.79	4%
Gull Creek	1.37	1.90	1.77	1.98	7.22	36%
Burroughs River	2.20	2.76	3.40	3.35	11.71	60%
Total	3.74	4.85	5.60	5.55	19.72	

The loss of meltwater from the basin by evaporation is not considered in Table 3. However, some idea of the significance of evaporation during the period of August 14 to 18 can be gotten from the heat balance data presented in Table 2. For the entire four days, it appears that only 465 langlys of heat energy was lost from the ice surface due to sublimation. Taking 600 cal g^{-1} as the latent heat of vaporization of water at $0^{o}C$, this would amount to about 0.7 cm of water evaporated, which is less than 4 percent of the total calculated melt for that period. It would appear then that loss due to evaporation is not very significant and can safely be ignored.

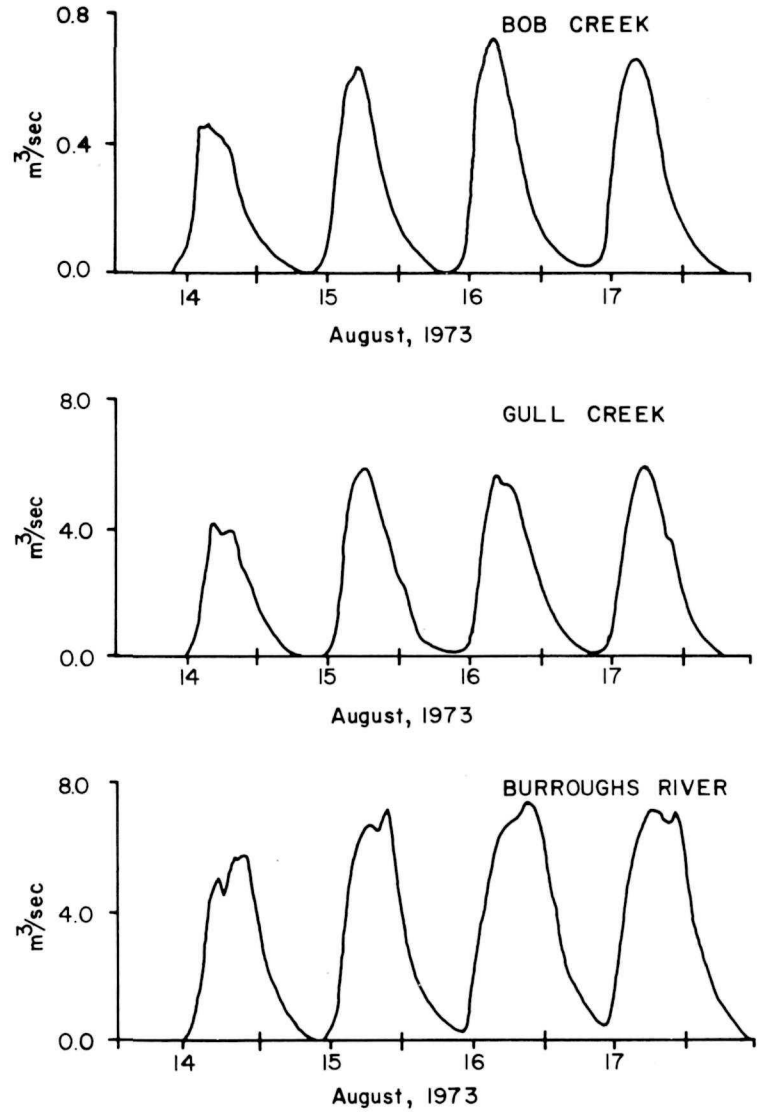

Figure 27. Meltwater runoff in Bob Creek, Gull Creek, and Burroughs River from August 14 through 17, 1973.

Sub-Basins of Burroughs Glacier

While studying the drainage of Mikkaglaciaren and Storglaciaren in northern Sweden, Stenborg (1973) observed that surficial structural features in the ice greatly control the direction of meltwater drainage. For example, he found that the oblique tensile crevasses in the ice often drain meltwater towards the glacier margins. In addition, he noted that drainage divides on the ice generally occur where two opposing systems of crevasses meet near the center line of the glacier.

In Figure 28, three sub-basins are shown for Burroughs Glacier. The drainage divides outlining each sub-basin are based on crevasse patterns on the glacier surface and on the observed flow direction of surficial streams draining meltwater. It appears that, on the upper part of the glacier, the flow of meltwater is controlled primarily by the strike direction of the transverse crevasses. Further down glacier, on the other hand, the longitudinal crevasses apparently control the direction of flow.

An attempt is made in Table 4 to compare the volume of melt, precipitation, and runoff for each sub-basin during the period from July 17 to August 26, 1973. The volume of melt in each sub-basin was calculated from ablation data shown in Figure 29 while the volume of precipitation was estimated by multiplying the rainfall recorded at the base camp during that period (10.1 cm) by the area of each sub-basin. The runoff from the sub-basins was determined from stream discharge data.

TABLE 4

WATER BALANCE FOR BURROUGHS GLACIER
JULY 17 - AUGUST 26, 1973

	Basin area km^2	Total rain $x10m^3$	Ice melt $x10m^3$	Total inflow $x10^6m^3$	Total outflow $x10^6m^3$
Bob Creek Basin	1.68	0.17	1.56	1.75	1.25
Gull Creek Basin	9.75	0.98	8.11	9.09	9.00
Burroughs River Basin	15.70	1.60	11.85	13.45	13.02
Totals	27.16	2.75	21.52	24.29	23.27

With the exception of Bob Creek sub-basin, Table 4 shows a reasonable agreement between the sum of melt and precipitation, and the outflow for each sub-basin. The imbalance recorded for Bob Creek sub-basin is probably due to recent changes in the position of the ice edge. When the base

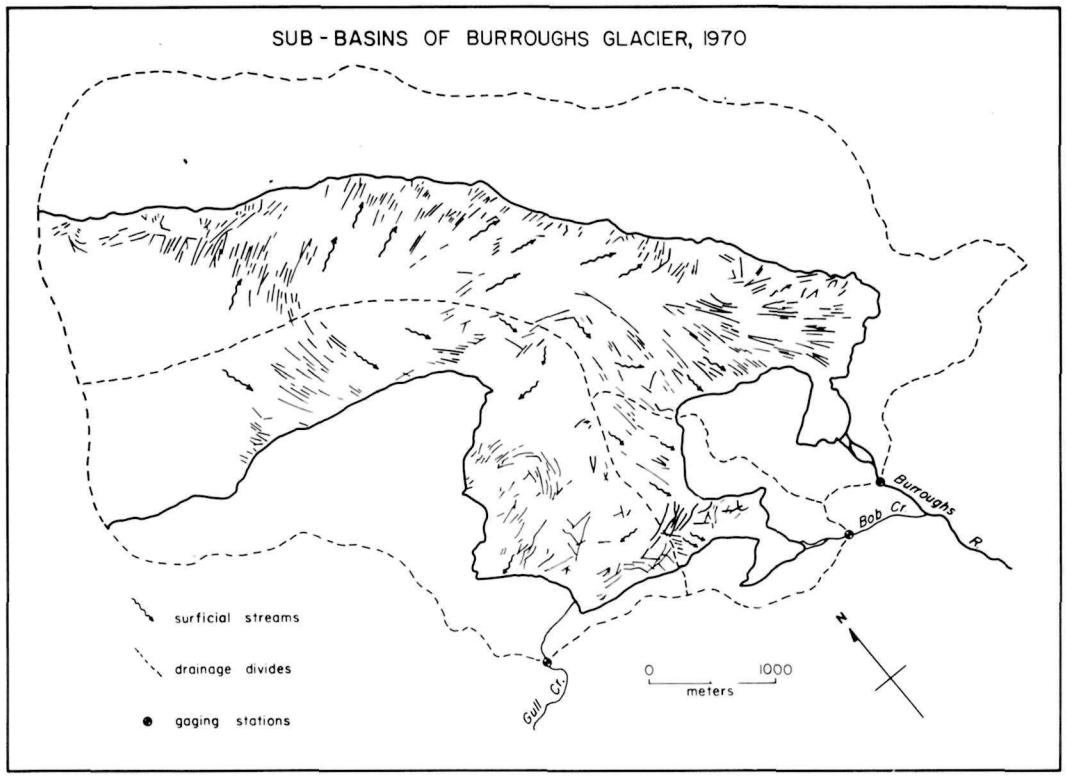
SUB - BASINS OF BURROUGHS GLACIER, 1970
surficial streams
drainage divides
gaging stations
0
1000
meters
N
Gull Cr.
Bob Cr.
Burroughs R.

Fig. 28

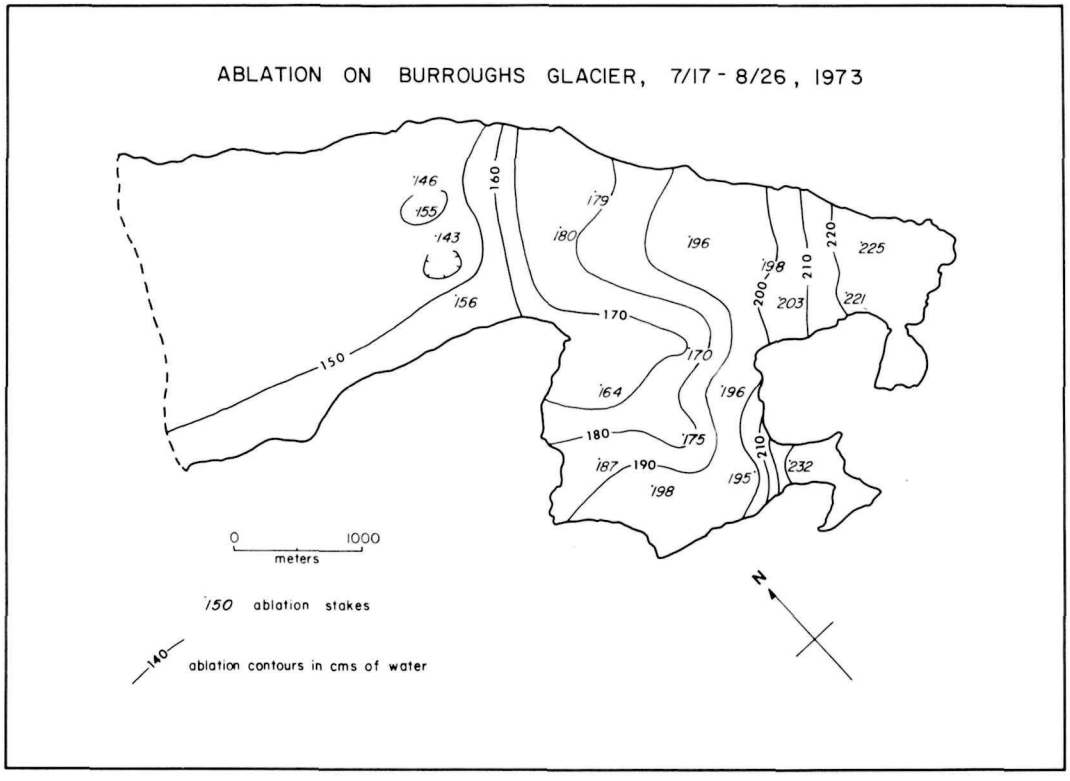
ABLATION ON BURROUGHS GLACIER, 7/17 - 8/26, 1973
146
155
143
156
150
160
179
180
196
198
200
210
220
225
203
221
170
170
164
196
180
175
187
190
198
195
210
232
0
1000
meters
150 ablation stakes
140 ablation contours in cms of water
N

Fig. 29

map was made in 1970, the extent of glacier ice in this area was considerably greater. Since then, however, the ice margin has retreated 10 to 100 m, effectively reducing the glacier-covered area by approximately 30 percent. Such a reduction in area would account for most of the imbalance for Bob Creek sub-basin. In the other two basins, where the glacier margin has not retreated as rapidly, the agreement is much better, which would suggest that the drainage divides drawn in Figure 28 are probably valid. The data also show that, for July 17 to August 26, precipitation accounted for just over 10 percent of the total outflow from the glacier.

MELTWATER STORAGE

The water balance of Burroughs Glacier for any interval of time can be expressed by the equation:

$$I - O = \Delta S,$$

where I is the inflow of meltwater, O is the outflow or runoff from the glacier, and ΔS is the change in meltwater storage within the glacier. In the previous two chapters estimates of the inflow and outflow based on global radiation receipts and runoff data have already been made for the period August 14 through 17, 1973. In this chapter, an analysis is made of the change in meltwater storage during this period and its relationship to the runoff from the glacier.

Change in Meltwater Storage

Figure 30 shows a record of both the inflow and outflow of meltwater for each sub-basin of Burroughs Glacier from 0000h August 14 to 0600h August 18. It is evident from these records that, during this period, a significant portion of the inflow was temporarily stored within each glacier sub-basin. In addition, the records show that the peak outflow from each sub-basin followed the peak inflow by approximately three to five hours. The change in storage within each sub-basin during the four days is shown by the curves presented in Figure 31. These curves were derived by calculating the difference between the hourly inflows and outflows presented in Figure 30. From the shape of the curves it is evident that, in the morning and afternoon of each day, when inflow exceeds outflow, storage in the sub-basins increases and reaches a maximum around 1600h to 1800h. In the evening and night, on the otherhand, when outflow exceeds inflow, meltwater is released from storage.

Storage Characteristics of Glacier Ice

Storage within each sub-basin of the glacier appears to occur in pools and channels on the glacier surface and in openings that develop in the ice itself. In particular, where the ice is heavily fractured or crevassed, meltwater readily passes through the ice and drains into a system of englacial passageways and tubes (Larson, 1977). A small amount of meltwater also collects in the drift deposits on and adjacent to the glacier, and in small lakes and ponds along the ice margin.

Shown in Table 5 is the meltwater balance for Burroughs Glacier from 0000h August 14 to 0600h August 18. The values given in the table for the inflow, outflow, and storage are in centimeters of water. It is evident from the data that during the 102 hour period, storage in the glacier sub-basins ranged from 2.6 to 6.9 cm. The average storage for the entire eastern tongue was approximately 3.6 cm. Most of this storage, however, was not observed on the glacier surface during this period, and therefore, it must be assumed that the bulk of the storage occurs within openings and passageways beneath the glacier surface.

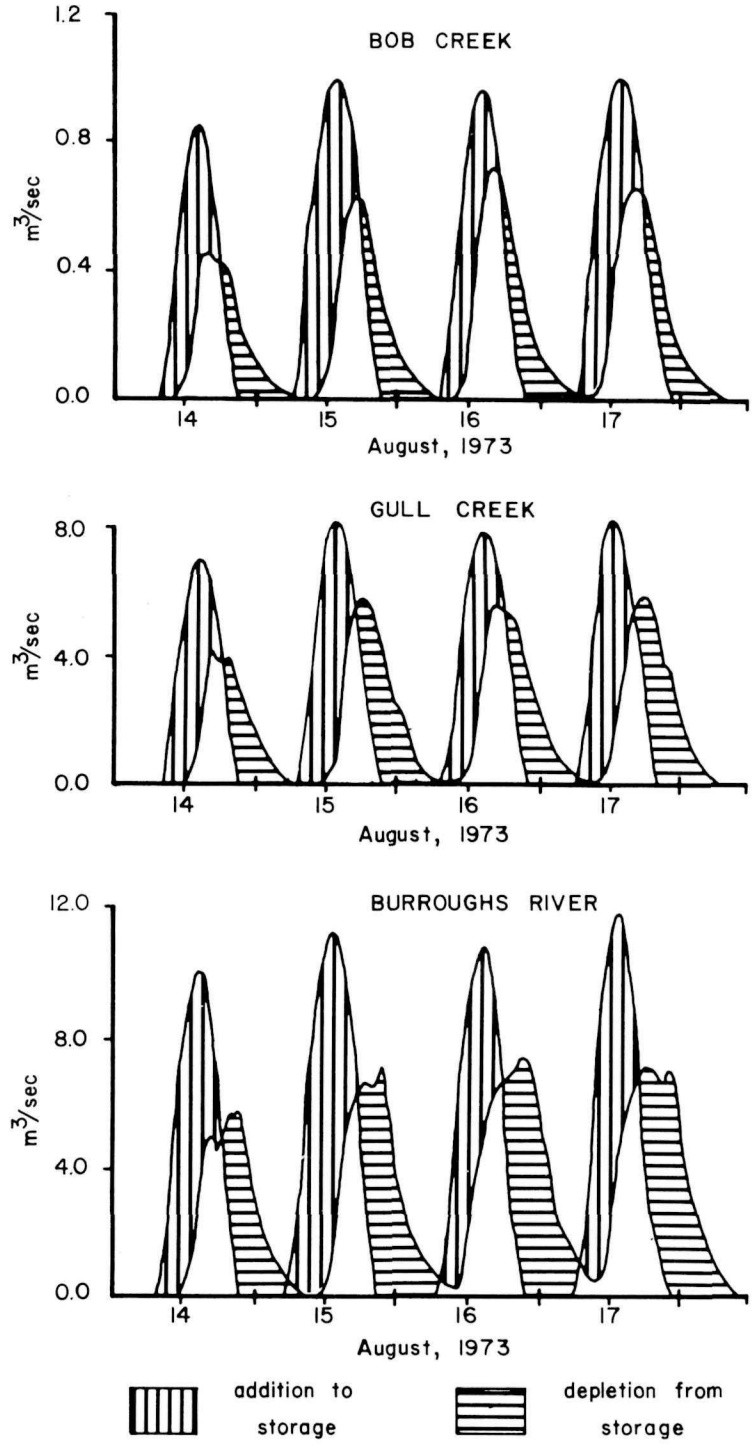

Figure 30. Inflow and outflow records for Bob Creek, Gull Creek, and Burroughs River sub-basins from August 14 through 17, 1973.

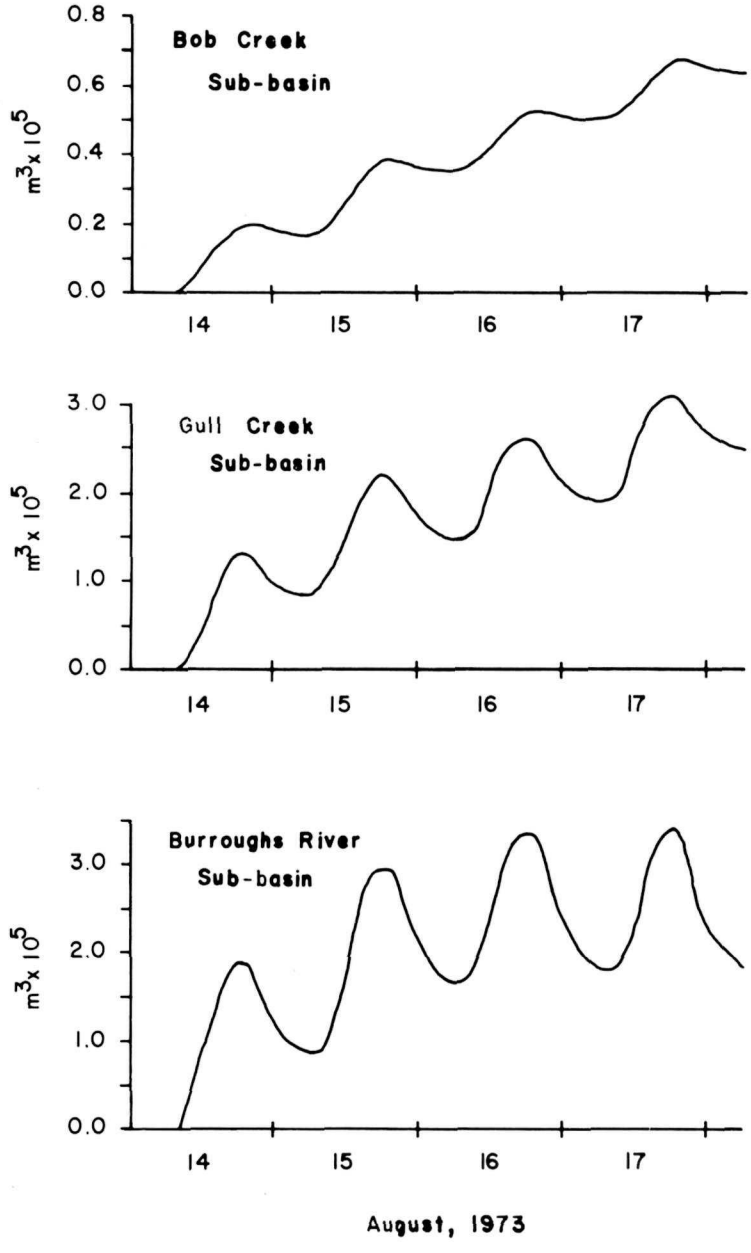

Figure 31. Curves showing change in meltwater storage in Bob Creek, Gull Creek, and Burroughs River sub-basins from August 14 through 17, 1973.

TABLE 5

MELTWATER BALANCE FOR BURROUGHS GLACIER

0000h August 14 - 0600h August 18

1973

		(cm of water)		
Sub-basin	ice area	inflow	outflow	storage
Bob Creek	0.89 km^2	15.7	8.8	6.9
Gull Creel	6.03 km^2	16.2	12.0	4.2
Burroughs River	6.98 km^2	19.4	16.8	2.6
Total	13.9 km^2	17.8	14.2	3.6

Relationship Between Storage and Runoff

When inflow is negligible, the outflow from a glacier, as in a storage reservoir, depend directly on the volume of meltwater in storage. This can be expressed by the equation:

$$dS = \tau dO,$$

where S is the storage, O is the outflow, and τ is a proportional constant equal to the reciprocal of the slope of the storage curve, and is used either as a constant or as a variable function of the outflow. The value also defines the average basin lag from the glacier to the channel control. For small and medium sized glaciers, Golubev (1973) found that τ generally varies linearly with the glacier area, and does not depend on the volume of water accumulated in storage.

Table 6 lists the average lag time τ calculated for each sub-basin of Burroughs Glacier during the period August 14 through 17. The values were obtained by a graphical method described by Golubev (1973). On the same time-discharge axis, the depletion segments of the daily outflow curves are plotted for the particular sub-basin in question (Fig. 32). Then, a low envelope curve is drawn to approximate the mean recession curve for the sub-basin. An integration of this curve provides the volume of accumulated water within the sub-basin:

$$S_{t_1} = \int_{t_2}^{t_1} O dt, \text{ where at } t_2,\ O_{t_2} = 0$$

The average basin lag τ is equal to $\tau = \frac{dS}{dO}$, but since a plot of accumulated

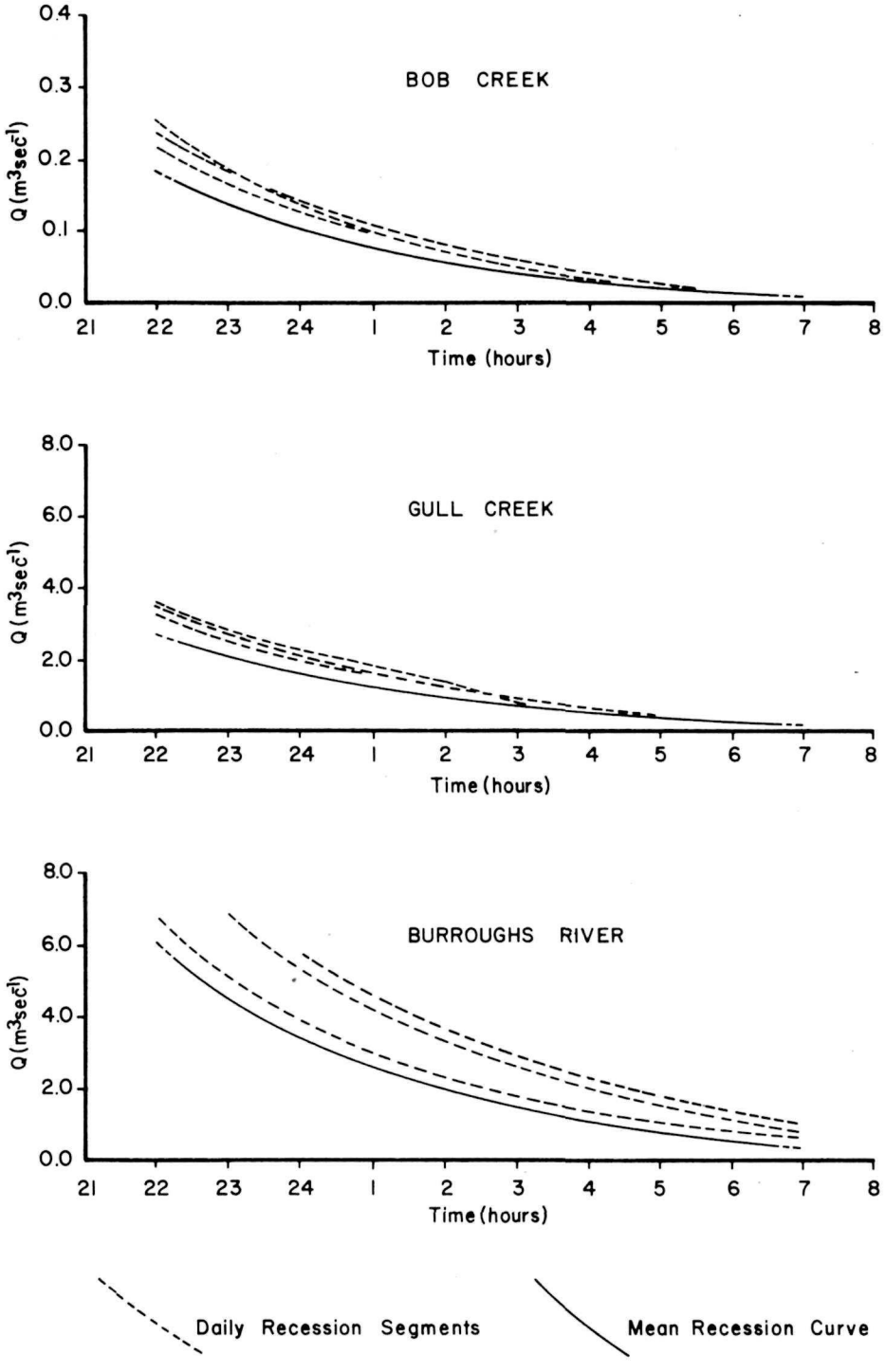

Figure 32. Graph showing daily recession curves and mean recession curves for Bob Creek, Gull Creek, and Burroughs River sub-basins.

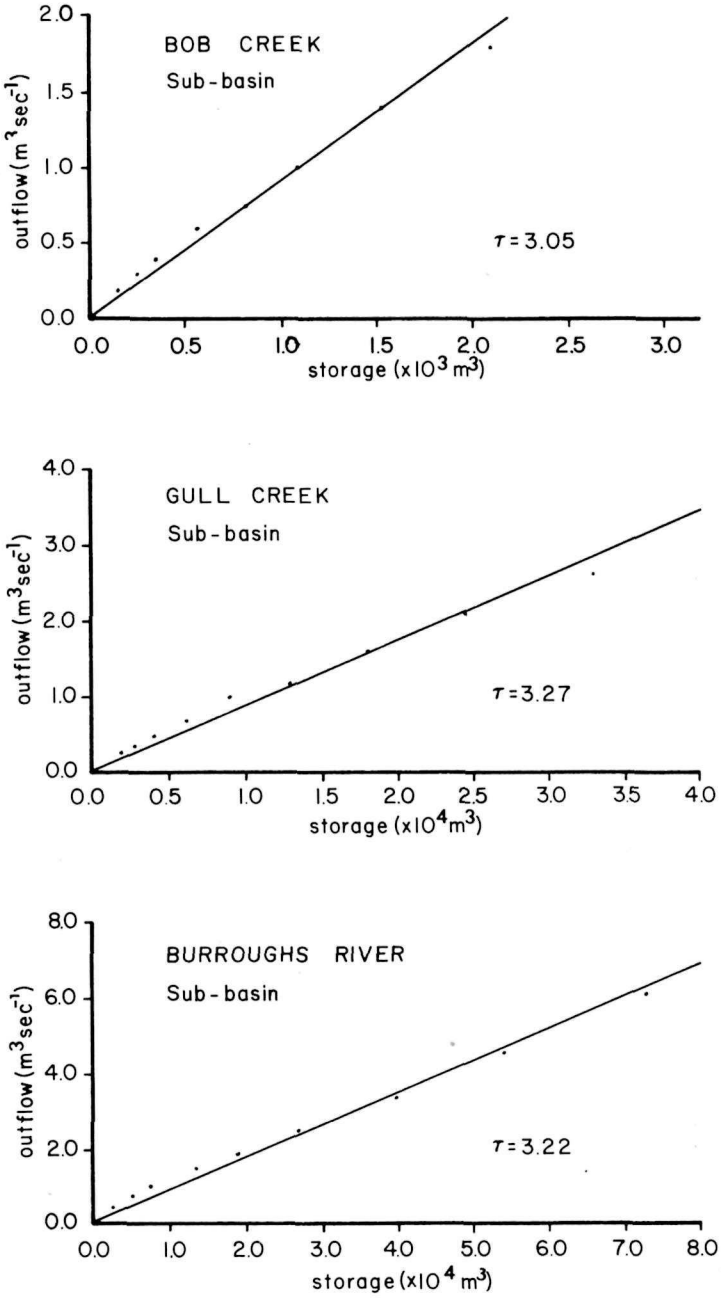

Figure 33. Plot showing relationship between storage and outflow for Bob Creek, Gull Creek, and Burroughs River sub-basins. Average basin lag τ is in hours.

water vs. outflow produces a quasilinear curve (Fig.), the average lag time for each sub-basin can be approximated by $\tau = \frac{S}{O}$.

TABLE 6

AVERAGE BASIN LAG
FOR BURROUGHS GLACIER

Sub-basin	Ice Cover (km^2)	Average Lag Time τ (Hours)
Bob Creek	0.89	3.05
Gull Creek	6.03	3.21
Burroughs River	6.98	3.22

From the data in Table 6, it is apparent that the average lag time in each sub-basin of Burroughs Glacier is about 3 hours. This value seems reasonable since peak outflow from each sub-basin generally follows the peak inflow by about 3 to 4 hours. It is interesting to note, also, that the average lag time for each sub-basin does not appear to depend greatly on the area of ice cover. This is probably because melt on the glacier is not uniform over the entire surface, but is concentrated mainly in the lower parts of the glacier, very near the outlet controls.

SUMMARY AND CONCLUSIONS

Burroughs Glacier is a wasting mass of neoglacial ice in southeastern Alaska. It covers approximately 26 km^2 and consists of two ice tongues emanating from a central ice divide. The highest point on the divide (475 m) lies well below the equilibrium line, so that no snow remains on the glaciers at the end of summer. The average rate of ice downwastage, recorded during 1972-73, was approximately 3.7 m yr^{-1}, with some local areas exceeding 8 m yr^{-1}. In places along the terminus of the glacier, backwastage of the ice measured as much as 200 m yr^{-1}. The flow velocity of the ice recorded at 18 points on the glacier surface ranged from 6 m yr^{-1} to less than 0.2 m yr^{-1}.

A hydrologic study made on the eastern tongue (13.9 km^2) of Burroughs Glacier during the summer of 1973 reveals that:

1) during clear sunny days, 57 to 69 percent of the heat-energy available for melting is from global radiation; the remaining sources of heat-energy are from convection between the ice surface and atmosphere (25-36%) and from condensation of water vapor on the ice surface (0-18%).

2) for the sunny period of August 14 through 17, the total inflow of meltwater into Burroughs Glacier, estimated from theoretical global radiation receipts, amounted to 24.24 x 10^5 m^3 (17.8 cm). The maximum rate of inflow into the ice was approximately 20 m^3 sec^{-1} (1.4 x 10^{-4} cm sec^{-1}).

3) sub-basins and drainage divides on the glacier can be defined and mapped on the basis of crevasse patterns. The eastern tongue of the glacier consists of three sub-basins, each of which is drained by an outlet stream.

4) The outflow of meltwater recorded in the outlet streams during the period August 14 through 17 amounted 19.72 x 10^5 m^3 (14.2 cm). The maximum rate of outflow to occur during that period was approximately 14 m^3 sec^{-1} (1.0 x 10^{-4} cm sec^{-1}).

5) the difference between the inflow and outflow from August 14 through 17 amounted to 4.52 x 10^5 m^3 (3.6 cm) of meltwater added to storage within the glacier. Most of this storage appears to be within fracture openings and channels in the ice itself.

6) the average basin lag τ for each sub-basin of the glacier was approximately 3 hours. There appears to be no direct correlation between the area of the sub-basins and the average lag time.

REFERENCES CITED

Ahlmann, H. W., 1948. Glaciological Research on the North Atlantic Coast: Royal Geog. Soc., Res. ser. 1, 83 p.

Ambach, W., 1960. Investigations of the heat balance in the area of ablation on the Greenland Ice Cap. Archiv. für Meteorologic, Geophysik and Beoklematologic, Series B, Bd. 10, Heft 3. p. 279-288.

Andrews, R. H., 1964. Meteorology and heat balance of the ablation area, White Glacier: Alex Heiberg Island Research Report No. 1, 107 p.

Colbeck, S. C., 1971. A theory of water percolation in snow: J. of Glaciology, v. 11, 1972, p. 369-385.

Cushing, H. P., 1891. Notes on the Muir Glacier region: Am. Geologist, v. 8, p. 207-230.

Cottier, R., and others, 1957. Die Hydroelektrisch en Analgin der Grande Dixence: Technischen Rundschau, Nr. 5, v. 1, 48 p.

de Brichambaut, P., 1963. Bayonnement Solaire et Echanges Radialifs Naturels. Paris, Gauthier Villars, 299 p.

Derikx, L., 1973. Glacial discharge simulation by groundwater analogue: Symposium on the Hydrology of Glaciers, Glaciological Society, Pub. No. 95.

Field, W. O., Jr., 1947. Glacier recession in Muir Inlet, Glacier Bay, Alaska Geog. Rev., v. 37, p. 349-399.

Garnier, B. J. and A. Ohmura, 1968. A method of calculating the direct shortwave radiation income of slopes: J. of Applied Meteor., 7, p. 796-800.

Goldthwait, R. P., 1966. Glacial history, in Misky, A., ed., Soil development and ecological succession in a deglaciated area of Muir Inlet, southeast Alaska: Ohio State University Inst. Polar Studies. Rept. 20, 18 p.

Golubev, G. N., 1973. Flow routing for a mountain glacier: Symposium on the Hydrology of Glaciers, Glaciological Society Pub. No. 95.

Grainger, M. and H. Lister, 1966. Wind speed, stability and eddy viscosity over melting ice surfaces: J. Glaciol. v. 6, no. 43, p. 101-128.

Halliner, G. J., and R. F. L. Martin, 1957. Dynamical and Physical Meteorology. New York and London, McGraw Hill Book Co., 470 p.

Havens, J. M., F. Muller and G. C. Wilmot, 1965. Comparative meteorological survey and a short-term heat balance study of the White Glacier: Axel Heiberg Island Research Reports, McGill University, No. 4, 68 p.

Hoinkes, H. and N. Untersteiner, 1952. Wärmeumsatz und ablation auf 1pengletschern I: Geografiska Annaler, v. 34, p. 99-158.

Keeler, C. M., 1964. Relationship between climate, ablation, and runoff on the Sverdrup Glacier, 1963, Devon Island N.W.T.: Arctic Institute of North America res. rept. no. 27, 80 p.

Kondratyev, K. Ya., 1969. Radiation in the Atmosphere. New York, Academic Press, 912 p.

Kotlyahov, V. M., 1973. On a possibility of artificial augmentation of melting by means of surface dusting on glacier (Experience of the Soviet Investigation): The role of snow and ice in hydrology, September 1972. Paris, UNESCO; Geneva, WMO; Budapest, IAHS.

Krimmel, R. M., W. V. Tangborn and M. F. Meier, 1973. The water flow through a temperate glacier: The role of snow and ice in hydrology. Proceedings of the Banff Symposia, September 1972. Paris, UNESCO; Geneva, WMO; Budapest, IAHS, p. 401-16.

Larson, G., 1977. The internal drainage of stagnant ice, Burroughs Glacier, Southeast Alaska: Ohio State Univ. Inst. Polar Studies, Rept. 65, 33 p.

Lister, H. and P. F. Taylor, 1961. Heat balance and ablation on an arctic glacier: Meddelelser om Grønland, Bd. 158, Heft 7, 54 p.

Loewe, F., 1966. Climate, in Mirsky, A., ed., Soil development and ecological succession in a deglaciated area of Muir Inlet, southeast Alaska: Ohio State Univ. Inst. Polar Studies, Rept. 20, p. 19-28.

Løken, O. H., 1970. Glacier Studies in the Canadian I.H.D. Program, Glaciers, Proceeding of Workshop Seminar 1970: Canadian National Committee--The International Hydrological Decade, p. 23-30.

Mackevett, E. M. Jr., D. A. Brew, C. C. Howly, L. C. Huff, and J. G. Smith, 1971. Mineral Resources of Glacier Bay National Monument, Alaska: U.S. Geol. Survey, Prof. Paper 632, 90 p.

McKenzie, G. D., 1968. Glacial history of Adams Inlet, Southeast Alaska: Ohio State Univ., Ph.D. Dissert., 200 p.

McKenzie, G. D., 1970. Glacial history of Adams Inlet, Southeastern Alaska: Ohio State Univ. Inst. Polar Studies, Rept. 25, 121 p.

Meier, M., 1969. Glaciers and Water Supply: American Water Works Association. v. 61, no. 1, pp. 8-12.

Meier, M., V. Wendell, L. Mayo, and A. Post, 1971. Combined Ice and Water Balance of Gulkana and Wolverine Glaciers, Alaska and South Cascade Glacier, Washington, 1965 and 1966 Hydrologic years: U.S. Geol. Survey Prof. Paper 715-A, 23 p.

Mickelson, D. M., 1971. Glacial geology of Burroughs Glacier Area, Southeastern Alaska: Ohio State Univ. Inst. Polar Studies Rept. 40, 149 p.

Ommanny, S., 1970. The Canadian Glacier Inventory, Glaciers, Proceeding of Workshop Seminar 1970: Canadian National Committee--The International Hydrological Decade, 4 p.

Östrem, G., 1971. Glaseologiske Undersokelser i Norge 1971, Rapport Nr. 2-71 fra Hydrologisk Avdelung: Norges Vassdrags - Or elektrisitetsvesen, Offset, 111 p. (with English summary).

Östrem, G., 1974. Glasiologiske undersokeler i Norge 1972, Rapport Nr. 1-74 fra Hydrologisk Avdelung: Norges Vassdrags - Og elektrisitetsvesen, Offset, 99 p., (with English summary).

Peterson, D.N., 1970. Glaciological investigations on the Casement Glacier, Southeast Alaska: Ohio State Univ. Inst. of Polar Studies Rept. no. 36, 115 p.

Post, A., D. Richardson, W. Tangborn, R. Rosselot, 1971. Inventory of Glaciers in the North Cascades, Washington: U.S. Geol. Survey Prof. Paper 705-A, 26 p.

Robin, G., 1958. Norwegian-British-Swedish Antarctic Expedition 1949-52, Scientific Results, v. 5, Glaciology III, Norsk Polarinstitutt, Oslo. 134 p.

Reid, H. F., 1892. Studies of Muir Glacier, Alaska: Nat'l Geog. Mag., v. 4, p. 19-84.

Sharp, R. P., 1951. Meltwater Behavior in Firn on Upper Seward Glacier St. Elias Mountains, Canada: Brussels Gen. Assembly. IAHS Pub. 32, p. 246-253.

Stenborg, T., 1973. Some Viewpoints on the Internal Drainage of Glaciers: Symposium on the Hydrology of Glaciers, Glaciological Society Publ. No. 95, p. 117-129.

Sverdrup, H. U., 1936. The eddy conductivity of the air over a smooth snow surface: (Scientific results of the Norwegian-Swedish Spitzbergen Expedition in 1934), Geofysiske Publikasjoner, v. 11, no. 7, 69 p.

Tangborn, V., 1966. Glacier Mass Budget Measurements by Hydrologic Means: Water Resources Res., v. 2, no. 1, p. 105-110.

Tangborn, V., R. Krimmel, and M. Meier, 1971. Comparison of Glacier Mass Balance by Glaciologic, Hydrologic and Mapping Methods, South Cascade Glacier, Washington: I.U.G.G. Moscow Assembly. IAHS Pub. No. 104.

Taylor, L., 1962. Ice Structures, Burroughs Glacier, southeast Alaska: Ohio State University Inst. Polar Studies, Rept. 3, 110 p.

Vivian, R., 1970. Hydrologic et Erosion Sous-Glaciaires: Rev. Geog. Alpine, v. 58, p. 241-269.

Wallen, C. C., 1948. Glacial-meteorological investigations on the Karsa Glacier in Swedish Lappland, 1942-48. Geografiska Annaler, v. 30, p. 451-572.

Wendler, G., and G. Weller, 1974. A heat-balance study on the McCall Glacier, Brooks Range, Alaska: A contribution to the international hydrological decade. J. of Glaciology, v. 13, no. 67, p. 13-26.

Williams, L. D., R. G. Barry, and J. T. Andrews, 1972. Application of computed global radiation for areas of high relief: J. of Applied Meteor., v. 11, p. 526-533.

APPENDIX A

List of Micrometeorological and Hydrological Equiptment

3 Steavens Water-level Recorders

1 Epply Pyronometer

3 Casello Hygrothermographs

3 Lambrecht Wind Recorders

1 Belfort Pyheliograph

1 USDA Standard Rain Gage

1 Gurley Current Meter

1 Gurley "pigmy" Meter

APPENDIX B

Hourly Values of Parameters in the Heat Balance Calculations

14 through 17, August 1973

l = hight (100cm)
u = hight (150cm)
U = wind (cm/sec)
T = temp. (°C)
E = vaprs. (mm Hg)
A = exchange coef.
Ql = latent heat (ly)
Qs = sensible heat (ly)
Ig = global rad. (ly)
Ra-Rs = long-wave rad (ly)

Date 8/14 Time	Uu	Ul	Tu	Tl	Eu	El	A	Ql	Qs	Ig	Ra-Rs
01:00	7.6	6.0	8.0	6.1	7.16	5.08	2.12	31.19	13.90	0.0	6.5
02:00	5.8	4.5	7.8	6.1	7.22	5.01	1.66	26.04	9.77	0.0	6.5
03:00	4.2	3.6	7.5	5.9	7.23	5.01	1.78	27.92	9.82	0.0	6.5
04:00	2.8	2.0	7.3	5.3	7.68	5.34	0.45	7.47	3.12	0.0	6.8
05:00	1.5	1.4	6.9	4.5	6.86	5.55	0.44	4.04	3.61	0.0	6.8
06:00	1.9	2.0	6.4	3.6	6.56	5.45	0.50	3.92	4.82	0.0	7.0
07:00	1.8	1.9	6.1	3.3	6.14	5.57	0.41	1.67	4.00	2.4	7.0
08:00	1.3	1.1	5.9	3.6	5.15	5.69	0.21	-.79	1.64	6.0	7.2
09:00	1.7	1.7	5.9	3.9	5.01	5.75	0.66	-3.45	4.55	12.0	7.2
10:00	1.4	1.5	6.1	4.5	4.87	5.89	1.06	-7.67	5.87	21.0	7.2
11:00	1.8	2.0	6.4	4.7	5.04	5.89	1.53	-9.24	9.01	38.4	7.2
12:00	2.7	2.7	6.9	4.7	5.22	5.50	1.17	-2.33	8.92	45.0	7.2
13:00	2.6	2.7	7.3	5.5	5.10	5.55	1.90	-6.05	11.81	48.0	7.2
14:00	2.4	2.6	7.8	6.1	5.31	5.36	2.35	-0.83	13.80	45.0	7.0
15:00	3.6	3.2	7.3	3.9	5.29	4.78	0.42	1.52	4.93	33.6	6.5
16:00	3.0	2.9	7.3	4.5	5.52	4.98	0.81	3.08	7.79	33.0	6.8
17:00	3.5	2.9	7.5	5.0	5.75	5.90	0.75	-.76	6.14	30.0	7.0
18:00	3.6	3.0	7.8	5.0	6.27	4.84	1.04	10.57	10.10	28.8	7.2
19:00	3.3	3.0	7.5	5.5	6.22	5.01	1.34	11.47	9.25	18.0	7.2
20:00	2.8	2.7	7.3	5.0	6.05	5.04	1.10	7.85	8.72	12.0	7.2
21:00	2.9	2.7	7.3	4.7	6.29	5.12	0.80	6.59	7.15	3.0	7.0
22:00	2.4	2.6	7.1	4.4	6.50	5.14	1.00	9.62	9.32	0.0	6.8
23:00	2.4	2.6	6.9	4.4	6.12	5.20	1.11	7.23	9.58	0.0	6.8
24:00	2.8	2.7	6.6	3.9	6.28	5.21	0.64	4.83	5.95	0.0	6.8
								133.89	183.57	452.2	166.6

Date 8/15 Time	Uu	Ul	Tu	Tl	Eu	El	A	Ql	Qs	Ig	Ra-Rs
01:00	2.5	2.4	6.4	3.9	5.91	5.20	0.63	3.15	5.42	0.0	6.8
02:00	2.3	2.5	6.4	3.9	5.91	5.45	0.91	2.97	7.87	0.0	6.8
03:00	2.1	2.1	6.1	3.5	5.93	5.18	0.48	2.57	4.35	0.0	6.8
04:00	1.3	1.6	6.1	3.5	6.07	5.30	0.65	3.55	5.85	0.0	6.8
05:00	2.0	2.3	5.9	3.5	5.99	5.30	0.88	4.31	7.32	0.0	6.8
06:00	2.3	2.3	6.1	3.9	5.93	5.32	0.79	3.41	6.01	0.0	7.0
07:00	1.8	1.8	6.1	4.5	5.86	5.43	1.04	3.18	5.77	0.6	7.2
08:00	0.9	1.0	6.4	5.0	5.69	5.43	0.96	1.77	4.66	6.0	7.2
09:00	1.4	1.3	6.9	5.8	4.92	4.91	1.01	0.07	3.85	21.0	7.2
10:00	1.5	1.6	7.3	6.4	4.68	4.90	2.11	-3.29	6.56	27.0	7.2
11:00	1.9	2.3	8.3	6.9	4.68	4.70	3.50	-0.50	16.94	42.0	7.2
12:00	2.4	2.5	8.7	7.2	3.46	3.73	2.50	-4.79	12.98	48.0	7.2
13:00	4.3	3.5	9.1	7.5	2.51	3.58	1.78	-15.52	9.86	54.0	7.2
14:00	3.5	3.4	9.6	7.8	2.51	3.65	2.64	-21.31	16.42	55.2	7.2
15:00	3.8	3.2	9.9	7.8	2.75	3.65	1.51	-9.65	10.99	51.0	7.2
16:00	4.5	3.6	9.9	7.8	2.92	3.73	1.48	-8.52	10.78	45.0	7.2
17:00	4.9	3.7	9.6	7.8	2.87	3.73	1.46	-8.92	9.11	36.0	7.2
18:00	5.5	4.2	9.6	7.2	2.96	3.73	1.28	-6.96	10.58	27.6	7.2
19:00	5.7	4.2	9.1	6.9	2.95	3.80	1.21	-7.27	9.18	18.0	7.2
20:00	5.2	4.0	8.9	6.4	2.99	3.75	1.06	-5.71	9.17	10.2	7.2
21:00	5.3	3.8	8.3	6.1	2.96	3.81	0.91	-5.45	6.88	6.0	7.2
22:00	3.5	2.9	7.5	6.1	3.11	3.81	1.48	-7.32	7.14	0.6	7.2
23:00	2.9	2.8	7.3	6.1	3.22	3.81	2.37	-9.91	9.83	0.0	7.2
24:00	3.5	3.1	7.1	6.1	3.33	4.02	2.31	-11.28	7.98	0.0	7.2
						Total		-99.39	205.51	537.8	170.6

Date 8/16 Time	Uu	Ul	Tu	Tl	Eu	El	A	Ql	Qs	Ig	Ra-Rs
01:00	2.8	2.5	7.3	6.1	3.37	3.96	1.72	-7.05	7.12	0.0	7.0
02:00	5.0	3.9	7.3	5.6	3.37	3.96	1.36	-5.09	8.01	0.0	6.8
03:00	5.3	4.0	7.3	5.6	3.45	4.09	1.28	-5.80	7.52	0.0	6.8
04:00	5.3	4.0	6.9	5.0	3.36	3.79	1.04	-3.16	6.81	0.0	6.8
05:00	5.8	4.4	6.9	5.0	3.38	3.92	1.16	-5.25	7.60	0.0	6.8
06:00	6.0	4.2	6.6	5.6	3.36	4.16	1.59	-9.02	5.50	0.0	7.0
07:00	5.4	4.1	7.1	5.6	3.40	4.16	1.48	-7.94	7.65	1.2	7.0
08:00	5.6	4.2	7.7	5.6	3.27	3.95	1.20	-5.76	7.85	7.2	7.0
09:00	5.5	4.2	7.8	6.1	3.15	3.95	1.49	-8.43	8.74	12.0	7.0
10:00	6.0	4.2	8.0	6.1	3.14	3.67	1.07	-4.03	7.05	19.2	7.0
11:00	5.2	4.0	8.2	6.7	2.94	3.85	1.70	-10.70	8.80	37.2	7.0
12:00	5.3	4.2	8.9	7.2	2.99	3.80	1.86	-10.68	10.93	45.0	7.0
13:00	5.8	4.1	9.6	7.8	2.96	3.89	1.36	-8.96	8.46	48.0	7.0
14:00	5.0	4.0	9.9	7.2	2.93	3.73	1.23	-6.96	11.47	54.0	7.2
15:00	5.5	4.2	9.6	6.7	2.96	3.68	0.98	-6.87	9.82	53.4	7.2
16:00	5.6	4.3	9.6	7.2	2.78	3.96	1.33	-11.08	11.00	44.4	7.2
17:00	5.9	4.4	9.9	7.8	2.84	3.73	1.50	-9.48	10.91	39.0	7.2
18:00	5.8	4.4	10.1	8.3	2.78	3.78	1.84	-13.02	11.43	24.0	7.2
19:00	6.1	4.6	10.1	7.8	2.69	3.65	1.50	-10.23	11.96	21.0	7.2
20:00	6.5	4.7	9.6	7.2	2.69	3.73	1.23	-9.09	10.23	12.0	7.2
21:00	6.2	4.6	9.2	6.7	2.79	3.68	1.16	-7.32	10.03	5.4	7.2
22:00	6.3	4.8	8.7	6.1	2.78	3.67	1.13	-7.13	10.17	1.2	7.2
23:00	6.3	4.8	8.7	6.1	2.85	3.81	1.41	-9.56	10.21	0.0	7.2
24:00	7.0	5.1	8.0	6.1	2.90	3.81	1.45	-9.36	9.53	0.0	7.2
						Total		-192.57	218.82	509.7	162.4

Date 8/17 Time	Uu	Ul	Tu	Tl	Eu	El	A	Ql	Qs	Ig	Ra-Rs
01:00	6.6	4.8	8.2	6.5	2.94	3.85	1.57	-10.11	9.22	0.0	6.5
02:00	6.0	4.6	8.7	6.7	2.87	3.82	1.56	-10.47	10.76	0.0	6.5
03:00	6.2	4.8	8.7	6.9	2.78	3.88	1.86	-14.47	11.56	0.0	6.5
04:00	5.9	4.7	8.7	6.9	2.84	3.88	1.96	-14.05	12.21	0.0	6.5
05:00	6.4	4.9	8.2	6.7	2.86	3.90	2.05	-15.13	10.65	0.0	6.5
06:00	6.8	4.8	7.8	6.1	3.02	3.88	1.38	- 8.39	8.10	0.0	6.5
07:00	6.2	4.5	7.8	5.8	3.10	4.01	1.16	- 7.45	7.99	1.2	6.8
08:00	5.8	4.4	7.8	6.1	3.10	4.09	1.53	-10.74	9.00	3.0	6.8
09:00	4.1	3.5	8.2	7.2	3.18	3.96	2.56	-14.13	8.84	18.0	7.2
10:00	4.0	3.4	8.7	7.8	3.21	3.97	2.65	-14.27	8.25	30.0	7.2
11:00	4.0	3.0	9.6	8.1	3.14	3.80	1.34	- 6.26	6.94	41.0	7.2
12:00	4.1	3.5	10.1	8.3	3.15	3.78	2.00	- 8.95	12.47	48.6	7.2
13:00	2.9	2.9	10.1	8.6	3.06	3.85	2.86	-16.03	14.85	51.0	7.2
14:00	3.3	3.2	10.5	8.9	3.05	3.93	2.89	-18.01	15.97	53.4	7.2
15:00	2.9	2.9	10.5	9.2	3.05	4.01	3.18	-21.63	14.29	51.6	7.2
16:00	3.0	3.0	11.0	10.3	3.15	4.13	4.20	-29.17	10.17	46.2	7.2
17:00	3.6	3.1	11.0	10.6	3.25	4.21	3.26	-22.19	4.51	39.0	7.2
18:00	4.6	3.4	11.0	10.0	3.25	4.05	1.92	-10.88	6.64	30.0	7.2
19:00	3.6	3.2	10.0	9.2	3.24	4.10	2.59	-15.75	11.62	21.0	7.2
20:00	3.2	3.0	9.6	8.1	2.60	3.97	2.43	-23.61	12.61	13.2	7.2
21:00	3.5	3.4	9.1	7.5	3.90	4.27	2.78	- 7.29	15.38	5.4	7.2
22:00	3.2	3.2	8.7	7.2	4.88	4.34	2.85	10.90	14.77	1.2	7.2
23:00	2.7	2.9	8.9	7.2	4.02	4.41	2.90	- 8.01	17.03	0.0	7.2
24:00	1.9	2.1	8.2	7.2	3.91	4.41	3.06	-10.85	10.59	0.0	7.2
						Total		-306.94	264.42	545.0	167.8

APPENDIX B

Hourly Values of Parameters in the Heat Balance Calculations

14 through 17, August 1973

l = hight (100cm)
u = hight (150cm)
U = wind (cm/sec)
T = temp. (°C)
E = vaprs. (mm Hg)
A = exchange coef.
Ql = latent heat (ly)
Qs = sensible heat (ly)
Ig = global rad. (ly)
Ra-Rs = long-wave rad (ly)

Date 8/14											
Time	Uu	Ul	Tu	Tl	Eu	El	A	Ql	Qs	Ig	Ra-Rs
01:00	7.6	6.0	8.0	6.1	7.16	5.08	2.12	31.19	13.90	0.0	6.5
02:00	5.8	4.5	7.8	6.1	7.22	5.01	1.66	26.04	9.77	0.0	6.5
03:00	4.2	3.6	7.5	5.9	7.23	5.01	1.78	27.92	9.82	0.0	6.5
04:00	2.8	2.0	7.3	5.3	7.68	5.34	0.45	7.47	3.12	0.0	6.8
05:00	1.5	1.4	6.9	4.5	6.86	5.55	0.44	4.04	3.61	0.0	6.8
06:00	1.9	2.0	6.4	3.6	6.56	5.45	0.50	3.92	4.82	0.0	7.0
07:00	1.8	1.9	6.1	3.3	6.14	5.57	0.41	1.67	4.00	2.4	7.0
08:00	1.3	1.1	5.9	3.6	5.15	5.69	0.21	-.79	1.64	6.0	7.2
09:00	1.7	1.7	5.9	3.9	5.01	5.75	0.66	-3.45	4.55	12.0	7.2
10:00	1.4	1.5	6.1	4.5	4.87	5.89	1.06	-7.67	5.87	21.0	7.2
11:00	1.8	2.0	6.4	4.7	5.04	5.89	1.53	-9.24	9.01	38.4	7.2
12:00	2.7	2.7	6.9	4.7	5.22	5.50	1.17	-2.33	8.92	45.0	7.2
13:00	2.6	2.7	7.3	5.5	5.10	5.55	1.90	-6.05	11.81	48.0	7.2
14:00	2.4	2.6	7.8	6.1	5.31	5.56	2.35	-0.83	13.80	45.0	7.0
15:00	3.6	3.2	7.3	3.9	5.29	4.78	0.42	1.52	4.93	33.6	6.5
16:00	3.0	2.9	7.3	4.5	5.52	4.98	0.81	3.08	7.79	33.0	6.8
17:00	3.5	2.9	7.5	5.0	5.75	5.00	0.75	-.76	6.14	30.0	7.0
18:00	5.0	3.0	7.8	5.0	6.27	4.84	1.04	10.57	10.10	28.8	7.2
19:00	3.3	3.0	7.5	5.5	6.22	5.01	1.34	11.47	9.25	18.0	7.2
20:00	2.8	2.7	7.3	5.0	6.05	5.04	1.10	7.85	8.72	12.0	7.2
21:00	2.9	2.7	7.3	4.7	6.29	5.12	0.80	6.59	7.15	3.0	7.0
22:00	2.4	2.6	7.1	4.4	6.50	5.14	1.00	9.62	9.32	0.0	6.8
23:00	2.4	2.6	6.9	4.4	6.12	5.20	1.11	7.23	9.58	0.0	6.8
24:00	2.8	2.7	6.6	3.9	6.28	5.21	0.64	4.83	5.95	0.0	6.8
								133.89	183.57	452.2	166.6

Date 8/15											
Time	Uu	Ul	Tu	Tl	Eu	El	A	Ql	Qs	Ig	Ra-Rs
01:00	2.5	2.4	6.4	3.9	5.91	5.20	0.63	3.15	5.42	0.0	6.8
02:00	2.3	2.5	6.4	3.9	5.91	5.45	0.91	2.97	7.87	0.0	6.8
03:00	2.1	2.1	6.1	3.5	5.93	5.18	0.48	2.57	4.35	0.0	6.8
04:00	1.3	1.6	6.1	3.5	6.07	5.30	0.65	3.55	5.85	0.0	6.8
05:00	2.0	2.3	5.9	3.5	5.99	5.30	0.88	4.31	7.32	0.0	6.8
06:00	2.3	2.3	6.1	3.9	5.93	5.32	0.79	3.41	6.01	0.0	7.0
07:00	1.8	1.8	6.1	4.5	5.86	5.43	1.04	3.18	5.77	0.6	7.2
08:00	0.9	1.0	6.4	5.0	5.69	5.43	0.96	1.77	4.66	6.0	7.2
09:00	1.4	1.3	6.9	5.8	4.92	4.91	1.01	0.07	3.85	21.0	7.2
10:00	1.5	1.6	7.3	6.4	4.68	4.90	2.11	-3.29	6.56	27.0	7.2
11:00	1.9	2.3	8.3	6.9	4.68	4.70	3.50	-0.50	16.94	42.0	7.2
12:00	2.4	2.5	8.7	7.2	3.46	3.73	2.50	-4.79	12.98	48.0	7.2
13:00	4.3	3.5	9.1	7.5	2.51	3.58	1.78	-13.52	9.86	54.0	7.2
14:00	3.5	3.4	9.6	7.8	2.51	3.65	2.64	-21.31	16.42	55.2	7.2
15:00	3.8	3.2	9.9	7.8	2.75	3.65	1.51	-9.65	10.99	51.0	7.2
16:00	4.5	3.6	9.9	7.8	2.92	3.73	1.48	-8.52	10.78	45.0	7.2
17:00	4.9	3.7	9.6	7.8	2.87	3.73	1.46	-8.92	9.11	36.0	7.2
18:00	5.5	4.2	9.6	7.2	2.96	3.73	1.28	-6.96	10.58	27.6	7.2
19:00	5.7	4.2	9.1	6.9	2.95	3.80	1.21	-7.27	9.18	18.0	7.2
20:00	5.2	4.0	8.9	6.4	2.99	3.75	1.06	-5.71	9.17	10.2	7.2
21:00	5.3	3.8	8.3	6.1	2.96	3.81	0.91	-5.45	6.88	6.0	7.2
22:00	3.5	2.9	7.5	6.1	3.11	3.81	1.48	-7.32	7.14	0.6	7.2
23:00	2.9	2.8	7.3	6.1	3.22	3.81	2.37	-9.91	9.83	0.0	7.2
24:00	3.5	3.1	7.1	6.1	3.33	4.02	2.31	-11.28	7.98	0.0	7.2
						Total		-99.39	205.51	537.8	170.6

Date 8/16											
Time	Uu	Ul	Tu	Tl	Eu	El	A	Ql	Qs	Ig	Ra-Rs
01:00	2.8	2.5	7.3	6.1	3.37	3.96	1.72	-7.05	7.12	0.0	7.0
02:00	5.0	3.9	7.3	5.6	3.37	3.96	1.36	-5.69	8.01	0.0	6.8
03:00	5.3	4.0	7.3	5.6	3.45	4.09	1.28	-5.80	7.52	0.0	6.8
04:00	5.3	4.0	6.9	5.0	3.36	3.79	1.04	-3.16	6.81	0.0	6.8
05:00	5.8	4.4	6.9	5.0	3.38	3.92	1.16	-5.25	7.60	0.0	6.8
06:00	6.0	4.2	6.6	5.6	3.36	4.16	1.59	-9.02	5.50	0.0	7.0
07:00	5.4	4.1	7.1	5.6	3.40	4.16	1.48	-7.94	7.65	1.2	7.0
08.00	5.6	4.2	7.7	5.6	3.27	3.95	1.20	-5.76	7.85	7.2	7.0
09:00	5.5	4.2	7.8	6.1	3.15	3.95	1.49	-8.43	8.74	12.0	7.0
10:00	6.0	4.2	8.0	6.1	3.14	3.67	1.07	-4.03	7.05	19.2	7.0
11:00	5.2	4.0	8.2	6.7	2.94	3.83	1.70	-10.70	8.80	37.2	7.0
12:00	5.3	4.2	8.9	7.2	2.99	3.80	1.86	-10.68	10.93	45.0	7.0
13:00	5.8	4.1	9.6	7.8	2.96	3.89	1.36	-8.96	8.46	48.0	7.0
14:00	5.0	4.0	9.9	7.2	2.93	3.73	1.23	-6.96	11.47	54.0	7.2
15:00	5.5	4.2	9.6	6.7	2.96	3.68	0.98	-6.87	9.82	53.4	7.2
16:00	5.6	4.3	9.6	7.2	2.78	3.96	1.33	-11.08	11.00	44.4	7.2
17:00	5.9	4.4	9.9	7.8	2.84	3.73	1.50	-9.48	10.91	39.0	7.2
18:00	5.8	4.4	10.1	8.3	2.78	3.78	1.84	-13.02	11.43	24.0	7.2
19:00	6.1	4.6	10.1	7.8	2.69	3.65	1.50	-10.23	11.96	21.0	7.2
20:00	6.5	4.7	9.6	7.2	2.69	3.73	1.23	-9.09	10.23	12.0	7.2
21:00	6.2	4.6	9.2	6.7	2.79	3.68	1.16	-7.32	10.03	5.4	7.2
22:00	6.3	4.8	8.7	6.1	2.78	3.67	1.13	-7.13	10.17	1.2	7.2
23:00	6.5	4.8	8.2	6.1	2.85	3.81	1.41	-9.56	10.21	0.0	7.2
24:00	7.0	5.1	8.0	6.1	2.90	3.81	1.45	-9.36	9.53	0.0	7.2
						Total		-192.57	218.82	509.7	162.4

Date 8/17											
Time	Uu	Ul	Tu	Tl	Eu	El	A	Ql	Qs	Ig	Ra-Rs
01:00	6.6	4.8	8.2	6.5	2.94	3.85	1.57	-10.11	9.22	0.0	6.5
02:00	6.0	4.6	8.7	6.7	2.87	3.82	1.56	-10.47	10.76	0.0	6.5
03:00	6.2	4.8	8.7	6.9	2.78	3.88	1.86	-14.47	11.56	0.0	6.5
04:00	5.9	4.7	8.7	6.9	2.84	3.88	1.96	-14.05	12.21	0.0	6.5
05:00	6.4	4.9	8.2	6.7	2.86	3.90	2.05	-15.13	10.65	0.0	6.5
06:00	6.8	4.8	7.8	6.1	3.02	3.88	1.38	- 8.39	8.10	0.0	6.5
07.00	6.2	4.5	7.8	5.8	3.10	4.01	1.16	- 7.45	7.99	1.2	6.8
08:00	5.8	4.4	7.8	6.1	3.10	4.09	1.53	-10.74	9.00	3.0	6.8
09:00	4.1	3.5	8.2	7.2	3.18	3.96	2.56	-14.13	8.84	18.0	7.2
10:00	4.0	3.4	8.7	7.8	3.21	3.97	2.65	-14.27	8.35	30.0	7.2
11:00	4.0	3.0	9.6	8.1	3.14	3.80	1.54	- 6.26	6.94	41.0	7.2
12:00	4.1	3.5	10.1	8.3	3.15	3.78	2.00	- 8.05	12.47	48.6	7.2
13:00	2.9	2.9	10.1	8.6	3.06	3.85	2.86	-16.05	14.85	51.0	7.2
14:00	3.3	3.2	10.5	8.9	3.05	3.93	2.89	-18.01	15.97	53.4	7.2
15:00	2.9	2.9	10.5	9.2	3.05	4.01	3.18	-21.63	14.29	51.6	7.2
16:00	3.0	3.0	11.0	10.3	3.15	4.13	4.20	-29.17	10.17	46.2	7.2
17:00	3.6	3.1	11.0	10.6	3.25	4.21	3.26	-22.19	4.51	39.0	7.2
18:00	4.6	3.4	11.0	10.0	3.25	4.05	1.92	-10.88	6.64	30.0	7.2
19:00	3.6	3.2	10.0	9.2	3.24	4.10	2.59	-15.75	11.62	21.0	7.2
20:00	3.2	3.0	9.6	8.1	2.60	3.97	2.45	-23.61	12.61	13.2	7.2
21:00	3.5	3.4	9.1	7.5	3.90	4.27	2.78	- 7.29	15.58	5.4	7.2
22:00	3.2	3.2	8.7	7.2	4.88	4.54	2.85	10.90	14.77	1.2	7.2
23:00	2.7	2.9	8.9	7.2	4.02	4.41	2.90	- 8.01	17.03	0.0	7.2
24:00	1.9	2.1	8.2	7.2	3.91	4.41	3.06	-10.85	10.59	0.0	7.2
						Total		-306.94	264.42	545.0	167.8